The American Journal of Pathology, Vol. 182, No. 2, February 2013

The American Journal of
PATHOLOGY
ajp.amjpathol.org

MUSCULOSKELETAL PATHOLOGY

The Anticancer Drug Tamoxifen Counteracts the Pathology in a Mouse Model of Duchenne Muscular Dystrophy

Olivier M. Dorchies,* Julie Reutenauer-Patte,* Elyes Dahmane,†‡ Hesham M. Ismail,* Olivier Petermann,* Ophélie Patthey-Vuadens,* Sophie A. Comyn,* Elinam Gayi,* Tony Piacenza,* Robert J. Handa,§ Laurent A. Décosterd,† and Urs T. Ruegg*

From the Department of Pharmacology, and the Geneva-Lausanne School of Pharmaceutical Sciences,‡ University of Geneva and University of Lausanne, Geneva, Switzerland; the Division of Clinical Pharmacology and Toxicology,† Innovation and Development Unit, Service of Biomedicine, Department of Laboratories, University Hospital of Lausanne, Lausanne, Switzerland; and the Department of Basic Medical Sciences,§ University of Arizona, Phoenix, Arizona*

Accepted for publication October 7, 2012.

Address correspondence to Olivier M. Dorchies, Ph.D., Department of Cell Biology, Sciences III, University of Geneva, 30 Quai Ernest-Ansermet, CH-1211 Geneva 4, Switzerland. E-mail: olivier.dorchies@unige.ch.

Duchenne muscular dystrophy (DMD) is a severe disorder characterized by progressive muscle wasting, respiratory and cardiac impairments, and premature death. No treatment exists so far, and the identification of active substances to fight DMD is urgently needed. We found that tamoxifen, a drug used to treat estrogen-dependent breast cancer, caused remarkable improvements of muscle force and of diaphragm and cardiac structure in the *mdx*^{5Cv} mouse model of DMD. Oral tamoxifen treatment from 3 weeks of age for 15 months at a dose of 10 mg/kg/day stabilized myofiber membranes, normalized whole body force, and increased force production and resistance to repeated contractions of the triceps muscle above normal values. Tamoxifen improved the structure of leg muscles and diminished cardiac fibrosis by ~50%. Tamoxifen also reduced fibrosis in the diaphragm, while increasing its thickness, myofiber count, and myofiber diameter, thereby augmenting by 72% the amount of contractile tissue available for respiratory function. Tamoxifen conferred a markedly slower phenotype to the muscles. Tamoxifen and its metabolites were present in nanomolar concentrations in plasma and muscles, suggesting signaling through high-affinity targets. Interestingly, the estrogen receptors ERα and ERβ were several times more abundant in dystrophic than in normal muscles, and tamoxifen normalized the relative abundance of ERβ isoforms. Our findings suggest that tamoxifen might be a useful therapy for DMD. *(Am J Pathol 2013, 182: 485–504; http://dx.doi.org/10.1016/j.ajpath.2012.10.018)*

Duchenne muscular dystrophy (DMD) is a common and fatal genetic disease that affects the striated muscles in boys. It is characterized by muscle wasting, starting at ~3 years of age, leading to progressive paralysis and loss of ambulation during the teenage years and cardiac dysfunctions that cause death in early adulthood.[1]

DMD results from the inability of muscles to express dystrophin, a large subsarcolemmal protein that bridges the extracellular matrix to the intracellular cytoskeleton. Dystrophin is essential for protecting muscle cells from contraction-induced mechanical damage and for regulating processes in the subsarcolemmal space, such as mechanotransduction, reactive oxygen species production, and cation channel activity. The absence of dystrophin causes calcium overload, oxidative stress, and impairment of mitochondrial functions, which, collectively, alter myofibrillar function and cause muscle cell death.[2,3] The ensuing chronic inflammation impairs muscle regeneration and renders the surviving fibers more susceptible to stress. The dystrophic muscles are progressively invaded by connective and adipose tissues,[1] resulting in a dramatic loss of muscle strength. Disease progression to the respiratory muscles [eg, the diaphragm (DIA)] and the heart greatly restricts the life expectancy of patients with DMD.[4,5]

Supported by Swiss National Science Foundation grant 3100A0-109981 (U.T.R.), REQUIP grant 326000-121314/1 (L.A.D.), the Duchenne Parent Project-The Netherlands (DPP-NL; S17474 DPP 2011-12), the Association Française contre les Myopathies (AFM; 13090, 13984, and 15093), and a Ph.D. student fellowship grant from the AFM (13091 to J.R.-P.).

Current address of O.M.D., Department of Cell Biology, University of Geneva, Geneva, Switzerland; of S.A.C., Centre for High-Throughput Biology, University of British Columbia, Vancouver, BC, Canada.

http://dx.doi.org/10.1016/j.ajpath.2012.10.018

So far, the only pharmacologic treatments that have been clinically validated for patients with DMD are the glucocorticoids, prednisolone, and deflazacort.[6] However, these drugs prolong muscle strength and ambulation of patients only for a short term,[6] and adverse effects lead some patients with DMD to discontinue treatment. The identification of additional pharmacologic compounds that would decrease the course of the disease remains a major goal for research.[7,8]

Estrogens have long been regarded as female sex hormones. The expression of the estrogen receptors (ERs) ERα and ERβ, which mediate most estrogen actions, and aromatase, the rate-limiting enzyme that produces estrogens from androgens, was found in skeletal muscle.[9–11] In fact, skeletal muscles are major sites of estrogen production in men and postmenopausal women. Overall, estrogens increase force output,[12] enhance muscle recovery from disuse atrophy,[13] protect skeletal muscle membrane from contraction-induced injury,[14] and reduce the risk of developing cardiovascular diseases.[15,16]

Selective estrogen receptor modulators (SERMs) are compounds that either mimic or antagonize estrogens in a tissue-dependent manner. Tamoxifen (TAM), a first-generation SERM with antiestrogenic activity on the mammary gland, has been used to prevent and treat breast cancers for >20 years. At the same time, its proestrogenic activity on bone has made it attractive for the treatment of osteoporosis.[17–19] TAM has shown efficacy in scavenging peroxyl radicals,[20] stabilizing biological membranes,[14] preventing apoptosis,[21] inhibiting fibrosis,[22,23] and modulating calcium homeostasis.[24–26] Because these features all contribute to the pathogenesis of DMD, we hypothesized that dystrophic muscles could benefit from chronic TAM treatment.

We found that oral administration of TAM at a dose of 10 mg/kg/day for 15 months to *mdx*^{5Cv} mice, a commonly used model for DMD, remarkably improved dystrophic muscle structure and function. Specifically, TAM improved the whole body force of living mice, increased the force of leg muscles above that of normal mice, rendered these muscles more resistant to fatigue, induced a shift toward a slower phenotype, stabilized muscle fiber membrane, and normalized their diameter. Importantly, TAM decreased the development of fibrotic tissue in the DIA and in the heart and considerably increased the amount of contractile muscle tissue in the DIA. All these effects were obtained with plasma and muscle concentrations of TAM and its active metabolites being in the low nanomolar range, well below the levels displayed by patients with breast cancer under standard TAM therapy (ie, 20 mg/day). ERα and ERβ proteins were both overexpressed several fold in dystrophic muscles, and TAM altered the relative abundance of the ERβ isoforms ERβ1 and ERβ2 at both the mRNA and at the protein levels. Because ERβ2 may function as an inhibitor of ERβ1 and the ERβ2-to-ERβ1 ratio partly controls ER signaling,[27,28] these alterations of ER levels are likely significant in the exceptional responsiveness of dystrophic muscles to TAM.

Because TAM has a good safety profile, not only in adults but also in children, our findings suggest that TAM might be helpful for the treatment of patients with DMD.

Materials and Methods

While this study was ongoing, we contributed to the elaboration of standard operating procedures for preclinical investigations in the dystrophic mouse.[29] Whenever possible, the present study was performed in accordance with the experts' recommendations.

Mice and Treatments

All procedures involving animals complied with the Swiss Federal Law on Animal Welfare. Colonies of dystrophic *mdx*^{5Cv} mice[30] (The Jackson Laboratory, Bar Harbor, ME), and wild-type (wt) C57BL/6J mice (Charles River France, Saint Germain sur l'Arbresle, France) were maintained at the School of Pharmaceutical Sciences. Mice were housed in plastic cages containing wood granule bedding, kept on a 12-hour dark/12-hour light cycle, and allowed unlimited access to food and water.

Tamoxifen [(Z)-tamoxifen, catalog number T-5648; Sigma-Aldrich, Buchs, Switzerland] was incorporated into standard rodent diet at 100 mg/kg (Provimi-Kliba, Kaiseraugst, Switzerland). Both control and TAM-containing pellets were stored at −20°C in 0.5-kg vacuum-sealed bags. Male pups were marked by microtattooing of the toes under slight ketamine-xylazine sedation. Three groups were treated for approximately 15 months (63 ± 1 week) starting on postnatal day 21, that is, at the time when necrosis starts in most leg muscles: 14 dystrophic males were given control diet (Dys group), 12 dystrophic males were given TAM-containing diet (TAM group), and 12 wt males were given control diet (wt group). Body weights and food consumption were monitored weekly. A group of 9 dystrophic females fed control diet (FEM group) was included for comparison of certain end points with the groups of male mice.

Wire Grip Test

After 58 to 60 weeks of treatment, a wire test was used to assess whole body force. The mice were allowed to grasp by their four paws a 2-mm diameter metal wire maintained horizontally 35 cm above a thick layer of soft bedding. The length of time until the mice fell from the wire was recorded. After each fall, the mice were allowed to recover for 1 minute. Each session consisted of three trials from which the scores were averaged. The final grid test score was calculated as the average value from three sessions performed at 1-week intervals.

Muscle Contraction Properties

At the end of the treatment period, mice were anesthetized, and muscle responses to electrical stimulations were recorded isometrically in the right triceps surae as previously

described.[31–36] At the end of the treatment period, mice were anesthetized by an i.p. injection of a mixture of urethane (1.5 g/kg) and diazepam (5 mg/kg). In brief, the knee joint was firmly immobilized, and the Achilles tendon was linked to a force transducer coupled to a LabView interface (National Instruments, Austin, TX). Two thin steel electrodes were inserted intramuscularly, and 0.5-ms pulses of controlled intensity and frequency were delivered. After manual settings of optimal muscle length (L_o) and optimal current intensity, five phasic twitches were recorded at a sampling rate of 3 kHz to determine the absolute peak twitch force (P_t), the time to peak twitch tension (TTP), the time for half relaxation from peak twitch tension ($RT_{1/2}$), the maximum rate of tension development (T_{dev}), and the maximum rate of tension loss (T_{loss}). After a 3-minute pause, muscles were subjected to a force-frequency test: 200-ms long stimuli of increasing frequencies (10 to 100 Hz by increments of 10 Hz) were delivered at intervals of 30 seconds. When necessary, further stimulations at 120, 150, and 200 Hz were delivered to obtain the maximum response, which was taken as the absolute optimal tetanic tension (P_o). After another 3-minute pause, the resistance of the triceps to repeated tetani was assayed. Frequency was set at 60 Hz, and muscle tension was recorded while stimulations were repeatedly delivered, each consisting of a 1-second burst and a 3-second rest. The responses were expressed as the percentage of the maximal tension. Absolute phasic and tetanic tensions were converted into specific tensions (in mN per mm^2 of muscle section) after normalization for the muscle cross-sectional area. The cross-sectional area values (in mm^2) were determined by dividing the triceps surae muscle mass (in mg) by the product of the optimal muscle length (in mm) and the density of mammalian skeletal muscle (1.06 mg/mm^3).

Tissue Collection and Plasma CK

Immediately after isometric force recording, heparin was injected into the heart (30 μL, 3000 IU/mL), the mice were bled, and plasma was prepared by centrifugation (1000 x *g*, 10 minutes, 4°C). Skeletal muscles and other selected organs were dissected and weighed. Plasma creatine kinase (CK) levels were determined with a commercial kit (Catachem; Investcare Vet, Middlesex, UK) according to the manufacturer's recommendations.

Quantification of TAM and of Its Metabolites

The concentrations of the TAM isomers (E)-TAM and (Z)-TAM, and the TAM metabolites (E)-4-hydroxytamoxifen (OH-TAM), (Z)-4-OH-TAM, (E)-*N*-desmethyl-TAM, (Z)-*N*-desmethyl-TAM, (E)-4-hydroxy-*N*-desmethyl-TAM, (Z)-4-hydroxy-*N*-desmethyl-TAM (endoxifen), in the plasma of the TAM-treated mice were determined by an ultra performance liquid chromatography–tandem mass spectrometry assay as described.[37] The levels of these compounds were also determined in the gastrocnemius (GAS) muscles from TAM-treated mice with the use of a modification of the method used for plasma. Briefly, the GAS muscles were pulverized in liquid nitrogen-cooled mortars. Twenty milligrams of the muscle powder was homogenized for 30 seconds with a tissue tearor (Omni International, Kennesaw, GA) in a mixture composed of 900 μL of absolute ethanol and 100 μL of deuterated internal standards solution (25 ng/mL TAM-d5, *N*-desmethyl-TAM-d5, 4-OH-TAM-d5, and 50 ng/mL endoxifen-d5, 1:1 E/Z mixture, in methanol). The tissue suspension was then centrifuged (4°C for 10 minutes at 16000 × *g*). Seven hundred microliters of the supernatant fluid was transferred into a propylene tube and dried under nitrogen at room temperature. The residue was reconstituted in 100 μL of acetonitrile, vortex-mixed, diluted with 200 μL of a buffer solution (10 mmol/L ammonium formate, containing 0.25% formic acid) and centrifuged again as above. Supernatant fluid (150 μL) was introduced in a high performance liquid chromatography glass microvial, and 20 μL was injected into the high performance liquid chromatography system. Ultra performance liquid chromatography–tandem mass spectrometry conditions (mobile phases, elution gradient, and mass spectrometer conditions) were identical to those described for plasma levels measurements.[37] Calibration curves for tissue samples, prepared in ethanolic matrix (20 mg tissue/mL), ranged from 0.05 to 3 ng/mL for (E)-endoxifen, 0.025 to 3 ng/mL for (Z)-endoxifen, and 0.013 to 3 ng/mL for (Z)-4-OH-TAM, (Z)-*N*-desmethyl-TAM, and (Z)-TAM. In this specific setting, the method was precise and accurate with the interassay precision (CV %) and accuracy (bias %) ranging between 1% and 13% and −8.9% and 6.1%, respectively.

For plasma and muscle sample, (E)-TAM, (E)-*N*-desmethyl-TAM, and (E)-4-OH-TAM levels were quantified with the calibration curves of their corresponding Z isomers. In plasma and tissue samples, E-TAM isomer was chromatographically identified by comparison of its retention time with that of the purchased pure standard (Toronto Research Chemicals Inc., North York, ON, Canada). (E)-*N*-desmethyl-TAM and (E)-4-OH-TAM isomers were tentatively identified by comparison of their retention times with those of E isomers produced *in vitro* by exposing methanolic solutions of the corresponding Z isomers to UV light (254 nm) for ∼3 hours.

The results are expressed as ng/mL of plasma, ng/g of tissue, and nmol/L. A qualitative analysis of the food pellets confirmed that (Z)-TAM was the only form of TAM in the TAM-containing diet and that the control diet was devoid of TAM and metabolites.

Histologic Examination of Skeletal Muscles and Morphometry

The extensor digitorum longus (EDL), GAS, soleus, and tibialis anterior (TA) muscles from the right leg and the right hemi-DIA were embedded in tragacanth gum, frozen in

liquid nitrogen-cooled isopentane, and stored at −80°C until processed further. Transverse sections 10 μm thick were stained with H&E according to standard procedures, and images covering the entire muscle sections were acquired either with a Spot Insight camera (Visitron Systems, Puchheim, Germany) mounted on an Axiovert 200M microscope (Zeiss, Feldbach, Switzerland) or with an Axiocam camera (Zeiss) fitted on a Mirax Midi automated microscope (Zeiss), at a final magnification of ×50 or ×200, respectively. In dystrophic mice, skeletal muscles undergo repeated cycles of necrosis and regeneration with progressive accumulation of adipose and connective tissues. In normal fibers, the nuclei are located close to the sarcolemma ("peripheral nuclei"), whereas in regenerated fibers the nuclei remain internalized. On the basis of these morphologic features, both normal and regenerated fibers were counted. Regenerated fibers are expressed as the percentage of the total muscle fibers.

Sections were incubated with 2 μg/mL wheat germ agglutinin conjugated to Alexa Fluor 488 (WGA-AF_{488}; Molecular Probes, Invitrogen, Basel, Switzerland) in phosphate-buffered saline for 1 hour at room temperature to stain the connective tissue as described.[36] Fluorescence images from the whole muscle surface were taken with a Mirax Midi microscope as described above. The area covered by the connective tissue was measured with the Metamorph software version 5.0r7 (Visitron Systems, Puchheim, Germany) and expressed as the percentage of the total muscle area. In addition, the minimum fiber diameter was determined in the GAS, DIA, EDL, TA, and soleus muscles with the use of the Metamorph software as described.[38] For each muscle >500 fibers were counted from four to six fields taken at a final magnification of ×200.

Fiber typing was performed by immunohistochemistry with the use of mouse monoclonal antibodies against specific myosin heavy chains (MyHCs), according to standard procedures. The primary monoclonal antibodies BA-D5, SC-71, BF-35, and BF-F3 (Developmental Studies Hybridoma Bank, Iowa City, IA) were used to reveal fibers expressing type I, type IIA, all types but IIX, and type IIB MyHCs, respectively. The BA-D5, SC-71, and BF-35 antibodies were detected with a goat anti-mouse IgG antibody conjugated to Alexa Fluor 594 (Molecular Probes), and the connective tissue was counterstained with WGA-AF_{488} as described above. The BF-F3 antibody was detected with a goat anti-mouse IgM antibody conjugated to Alexa Fluor 488 (Molecular Probes). Fibers of type I and of type IIA were counted on separate sections. Other sections were double-stained with the anti-type IIB and all anti-types but IIX as above, and the connective tissue was counterstained with WGA-AF_{594} (Molecular Probes). The negative fibers were classified as IIX, and the yellow fibers (resulting from the superimposition of the green and red staining) were classified as IIB. The number of fibers expressing a given MyHC was determined with ImageJ version 1.46r (NIH, Bethesda, MD) from the whole TA, EDL, and soleus muscles, from the right hemi-DIA, and from the lateral GAS muscle and was expressed as the percentage of the total fiber count.

Further morphometric analyses were performed on the right hemi-DIA after H&E staining as follows. Approximately 10 images at a final magnification of ×100 were needed to capture the whole surface. Each image was viewed with ImageJ software, and lines were drawn at three preset locations equally distributed perpendicularly to the long axis of the DIA. At these locations, the thickness of the DIA was measured, and the number of myofibers crossing these lines was counted. The adipose tissue was identified as unstained "empty" fibers demarcated by perimysial connective structures. The foci of adipose tissue were demarcated with Photoshop software version 7.0 (Adobe, San Jose, CA). Then, the corresponding areas were quantified with ImageJ software and expressed as the percentage of the total muscle area. An approximate value of the area occupied by muscle cells (both normal and regenerated fibers) in the DIA was obtained by subtracting the surfaces of adipose and connective tissues from the total muscle surface.

Determination of Cardiac Fibrosis

Hearts were fixed in 4% buffered paraformaldehyde. After inclusion in paraffin, 5-μm-thick sections across the ventricles were collected 1.50 mm, 2.25 mm, and 3.00 mm from the apex and stained with Masson trichrome. The entire cross-sections were microphotographed with a Mirax Midi microscope at a final magnification of ×200. Each virtually reconstructed section was divided into four images from which the area covered by fibrotic deposits (appearing as a blue staining on a red background) was quantified with ImageJ software and expressed as the percentage of the total tissue surface. Finally, the values obtained from the three sections were averaged.

ER mRNA Expression

The left GAS muscle was snap-frozen in liquid nitrogen and stored at −80°C until processed. The muscles were ground to a fine powder in mortars cooled in liquid nitrogen. RNA were extracted from 10 mg of muscle powder (RNeasy Fibrous Tissue mini kit; Qiagen, Hombrechtikon, Switzerland), and 100 ng of total RNA was reverse-transcribed with Super-Script II Reverse Transcriptase (Invitrogen). The cDNA corresponding to 1 ng of reverse-transcribed total RNA was subjected to quantitative PCR (qPCR) amplification with the use of SYBR detection. To quantify the overall ERα or ERβ variants, primers were designed in regions that are not affected by alternative splicing. The expression levels of ERα and ERβ relative to the levels in the Dys group were determined with the TATA box-binding protein (*TBP*) as the invariant housekeeping gene.

The identification of the ERβ mRNA variants encoding the ERβ1, ERβ2, ERβ5, ERβ5A, and ERβ6 isoforms (as defined under the Accession number O08537 of the

UniProtKB/Swiss-Prot database) in the GAS muscle was performed by PCR as described.[39] Briefly, 1 μL of GAS muscle cDNA was subjected to PCR amplification with the use of primers annealing to exons 5 and 10 and under the following conditions: 95°C for 60 seconds; 40 cycles consisting of 95°C for 20 seconds, 55°C for 30 seconds, and 72°C for 60 seconds; and a final elongation step at 72°C for 5 minutes. As positive controls, mRNA from ovaries and brain were run in parallel. Three microliters (GAS muscle) or 0.1 μL (ovary) of the PCR product was resolved on denaturing polyacrylamide-urea gels (5W, 2 hours, 57°C) as described.[39] After silver staining, the gels were air-dried between two sheets of cellophane and scanned, and densitometric analysis of the signals was performed with ImageJ software. Alternatively, 1000-fold dilutions of the PCR products were used as templates for a second round of PCR amplification with the use of primers hybridizing to exons 6 and 8. The conditions were as described above, except that 35 cycles were performed and the annealing temperature was set to 60°C. Ten microliters (GAS muscle), 3 μL (brain), or 0.3 μL (ovary) of the second PCR products were resolved on 1.2% agarose gels and stained with ethidium bromide before quantification of ERβ1 and ERβ2 signals.

The primers used are shown in Table 1. They were designed from the sequences published under the NCBI Accession numbers NM_007956.4 (mouse ERα), NM_010157.3 (mouse ERβ1), NM_207707.1 (mouse ERβ2), and NM_013684.3 (mouse TATA box-binding protein).

Protein Expression

Muscle extracts were prepared from the left GAS muscle powder as described.[34] The final protein concentration was adjusted to 3 μg/μL with reducing Laemmli buffer. Muscle extracts (30 to 60 μg/lane) were resolved by SDS-PAGE, and proteins were transferred onto nitrocellulose membranes according to standard procedures. Equal loading and transfer efficiency were verified by staining with Ponceau Red. Membranes were blocked for 1 hour in TBST (20 mmol/L Tris-base, 150 mmol/L NaCl, 0.1% Tween-20, pH 7.5) containing 5% nonfat dry milk and incubated overnight at 4°C with a primary antibody (see Table 2 for detailed information on the primary antibodies used, providers, clonality, working dilutions, and nature of the competing protein). After extensive washing, membranes were incubated for 1 hour with an appropriate horseradish peroxidase-conjugated secondary antibody in TBST containing 5% milk. The bound antibody against ERβ2[27] was detected with protein G—horseradish peroxidase in TBST-milk. Proteins were revealed by chemiluminescence (ECL plus kit; Amersham, GE Healthcare Europe, Glattbrugg, Switzerland) after exposure to Fuji X-ray films (Fujifilm Europe, Dusseldorf, Germany). The films were scanned, and densitometric analysis was performed with ImageJ software. Signals were normalized to the MyHC content (determined on separate gels stained with Coomassie Blue) and corrected for the intensity of a reference sample loaded several times on every gel for the purpose of intragel and intergel comparisons.[34]

Data and Statistical Analysis

One wt mouse and one Dys mouse died at 55 and 64 weeks of age, respectively. Two Dys mice, one TAM mouse, and one FEM mouse died on preterminal anesthesia. Thus, the data presented here were collected from 11 to 14 males and from 8 to 9 females and expressed as the means ± SEMs. GraphPad Prism software version 5.03 (GraphPad, San Diego, CA) was used for constructing the graphs and for performing the statistical analyses. The differences between groups were assessed by one-way analysis of variance followed by Tukey's multiple comparison posttest. Differences with P values ≤ 0.05 were considered significant.

Results

Effects of TAM Treatment on Mouse Behavior, Body Weight, and Food Intake

The mice did not show noticeable alterations of their behavior during the 15 months of TAM treatment. Overall,

Table 1 Primers used for analysis of estrogen receptor mRNA levels

Primer	Exon	Sequence	Amplicon size (bp)
Primers used for determination of ER levels by RT-qPCR			
ERα-forward	5	5′-TGCGCAAGTGTTACGAAGTG-3′	
ERα-reverse	6	5′-TTTCGGCCTTCCAAGTCATC-3′	109
ERβ-forward	2	5′-TCGCTTCTCTATGCAGAACC-3′	
ERβ-reverse	3	5′-AGAAGTGAGCATCCCTCTTG-3′	138
TBP-forward	6	5′-TGCTGCAGTCATCATGAG-3′	
TBP-reverse	7	5′-CTTGCTGCTAGTCTGGATTG-3′	115
Primers used for determination of ER levels by RT-qPCR			
ERβ-forward	5	5′-TGAAGGAGCTACTGCTGAAC-3′	
ERβ-reverse	10	5′-CCCACTTCTGACCATCATTG-3′	914, 860, 726, 721, 587*
ERβ-forward	6	5′-GCTGATGGTGGGGCTGATGT-3′	
ERβ-reverse	8	5′-ATGCCAAAGATTTCCAGAAT-3′	177, 123†

*Amplicons corresponding to ERβ2, ERβ1, ERβ6, ERβ5, and ERβ5A isoforms, respectively.
†Amplicons corresponding to ERβ2 and ERβ1 isoforms, respectively.

Table 2 Characteristics of the antibodies used for analysis of protein levels

Antigen	Host	Clonality	Clone	Dilution	Competitor	Company	Catalog no.
α7 Integrin*	Rat	M	Cy8	1:2000	BSA	NA	NA
αB-crystallin	Rabbit	P	NA	1:1000	BSA	Calbiochem	238702
Calcineurin	Rabbit	P	NA	1:1000	BSA	Cell Signaling Technology	2614
Calsequestrin 1	Mouse	M	VIIID12	1:3000	BSA	Thermo Scientific	MA3-913
Calsequestrin 2	Rabbit	P	NA	1:2000	BSA	Thermo Scientific	PA1-913
ERα	Rabbit	P	NA	1:400	Milk	Santa Cruz Biotechnology	sc-7207
ERβ1	Rabbit	P	NA	1:1000	BSA	Cell Signaling Technology	5513
ERβ2	Rabbit	P	Twoβer.1†	1:1000	BSA	NA	NA
Parvalbumin	Mouse	M	NA	1:2000	BSA	Millipore	MAB1572
SERCA1	Mouse	M	IIH11	1:2000	BSA	Thermo Scientific	MA3-911
SERCA2	Rabbit	P	NA	1:1000	BSA	Abcam	ab3625
Utrophin	Mouse	M	DRP3/20C5	1:1000	Milk	Novocastra	NCL-DRP2

*Kindly donated by Prof. Randall H. Kramer (University of California, San Francisco, CA).
†Described previously.[27]
BSA, bovine serum albumin; M, monoclonal; NA, not applicable; P, polyclonal.

the groups of untreated Dys males and of untreated wt males showed similar growth curves (Supplemental Figure S1A). The mice treated with TAM for 15 months (TAM) were significantly smaller throughout the study and, at sacrifice they weighed the same as the untreated dystrophic females (FEM; Supplemental Figure S1, A and B). From the food consumption curves (Supplemental Figure S1C), we calculated that TAM intake decreased from 14 to 10 mg/kg/day during the first 17 weeks of treatment and then remained at ∼10 mg/kg/day until the end of the study.

Effects of TAM Treatment on the Weight of Organs and Muscles

The Dys mice had larger livers and testes than the wt mice. TAM treatment fully normalized the relative weights of these organs (Supplemental Table S1). The mice in the TAM group had significantly less white fat and more brown fat than the untreated Dys mice (Supplemental Table S1). TAM treatment did not change the relative weights of the other organs examined, such as the heart and the kidneys.

The Dys mice exhibited a significant hypertrophy of all of the skeletal muscles examined (Supplemental Table S1), which is a common feature of the dystrophic mouse models. Hypertrophy of the GAS, plantaris, soleus, and TA muscles was partly rescued by TAM. The relative weight of the triceps surae was completely normalized (Table 3). Overall, TAM diminished the relative weights of the muscles close to those of FEM mice, which showed less hypertrophy than the Dys group. In marked contrast, TAM increased the weight of the EDL muscle and the DIA. The relative weights of the heart were similar in all groups.

Table 3 Effect of TAM treatment on the mechanical properties of the triceps muscle

	Dys	TAM	wt	FEM
Phasic and tetanic isometric tensions				
P_t, actual (mN)	902.0 ± 39.2	1001.5 ± 127.2	1192.8 ± 35.7**	516.6 ± 19.0***†††
P_t, specific (mN/mm^2)	81.9 ± 2.9	162.3 ± 16.6***	109.9 ± 3.3*†	66.1 ± 2.4†††
P_o, actual (mN)	3013 ± 160	2835 ± 85	4573 ± 197***†††	2108 ± 66***†††
P_o, specific (mN/mm^2)	273.9 ± 11.3	465.4 ± 9.3***	421.0 ± 16.8***†	269.3 ± 6.7†††
Kinetics of contraction and relaxation				
TTP (ms)	14.9 ± 0.3	23.2 ± 1.5***	16.4 ± 0.3*†††	15.1 ± 0.6†††
$RT_{1/2}$ (ms)	15.9 ± 0.5	27.3 ± 1.1***	16.9 ± 0.4†††	18.1 ± 1.2†††
T_{dev} (%max/ms)	14.75 ± 0.50	9.42 ± 0.77***	15.28 ± 0.31†††	13.83 ± 0.68†††
T_{loss} (%max/ms)	4.09 ± 0.25	2.53 ± 0.16***	4.15 ± 0.18†††	3.37 ± 0.26†
Structural characteristics of the triceps surae				
Mass, actual (mg)	190.2 ± 3.4	112.1 ± 4.3***	189.0 ± 3.8†††	131.7 ± 3.6***†
Mass, corrected (mg/g)	5.26 ± 0.11	4.43 ± 0.12***	4.70 ± 0.09***	4.47 ± 0.11***
L_o (mm)	16.40 ± 0.19	17.28 ± 0.20**	16.41 ± 0.20††	15.86 ± 0.17†††
CSA (mm^2)	10.95 ± 0.22	6.12 ± 0.20***	10.87 ± 0.19†††	7.84 ± 0.21***

Data represent means ± SEMs from 8 to 11 mice.
*$P \leq 0.05$, **$P \leq 0.01$, and ***$P \leq 0.001$ compared with the Dys group.
†$P \leq 0.05$, ††$P \leq 0.01$, and †††$P \leq 0.001$ compared with the TAM group.
CSA, cross-sectional area; L_o, optimal muscle length; P_o, optimal tetanic tension; P_t, peak twitch tension; T_{dev}, tension development; T_{loss}, tension loss; TTP, time to peak twitch tension.

Effect of TAM Treatment on the Wire Test Performance

Within the last weeks of the treatment period, a wire test was used to assess whole body force. Typically, soon after the mice were allowed to grasp the horizontal wire, they started to move along the wire and tried to flip around their body's axis to explore the wire in the other direction (Figure 1A). The Dys animals rapidly lost the grip of their hind paws, causing them to hang onto the wire with their fore limbs only. From this position, the mice were rarely able to bring their hind paws back onto the wire and were unable to sustain their own body weight for more than a few seconds at each testing (Figure 1A). By contrast, both the wt and the TAM mice were able to move their fore limbs and chest into an extended position over the wire, to bring their hind limbs back onto the wire, and to turn around their body's axis to flip from one direction of the wire toward the other. The TAM group performed much better than the Dys group and equally well as the wt group (Figure 1B). The FEM group performed significantly better than the Dys group but remained significantly weaker than the TAM group. Given that the smaller body weight of the dystrophic females and TAM-treated males could increase their score at the wire test, we also expressed the physical impulse as the product of the wire test score (in seconds) and the mouse body weight (in g).[40] The improved performance of the TAM group compared with the Dys group was still marked, whereas the FEM group performed as poorly as the Dys group (Figure 1C).

Effect of TAM Treatment on Plasma CK Activity

Plasma CK activity was approximately three times higher in dystrophic males than in normal males, revealing an increased fragility of dystrophic muscle membrane (Figure 2). CK levels were much lower in dystrophic females than in dystrophic males, suggesting a role for estrogens in stabilizing muscle membranes. TAM treatment reduced plasma CK levels to values not significantly different from those of normal males and of dystrophic females (Figure 2).

Effects of TAM Treatment on Muscle Contractile Properties

The isometric contractile characteristics of the triceps surae muscle were determined at the end of the treatment period. The muscle mechanics data are summarized in Table 3 and the most remarkable findings are shown in Figure 3. After correction for the body weight, the dystrophic triceps presented a slight hypertrophy compared with wt triceps. This was normalized by TAM (Table 3). Both phasic tension (P_t) and tetanic tension (P_o) were reduced in dystrophic mice compared with normal mice. Although the actual size of the triceps of the TAM group was reduced compared with the Dys group, the P_t and P_o outputs were similar in both groups (Table 3). Correction for the muscle cross-sectional area showed that the P_t and P_o developed by the TAM-treated mice were considerably higher than those of the untreated Dys mice (Figure 3, A and C). In fact, TAM treatment for 15 months increased the specific P_t and P_o of the dystrophic triceps by 100% and 70%, respectively. Remarkably, the triceps of TAM-treated mice became significantly stronger per surface unit than those of normal mice (Table 3 and Figure 3, A and C).

The time required to achieve maximum contraction (TTP) was slightly longer in the wt group than in the Dys group, whereas the time for $RT_{1/2}$ was similar in both groups

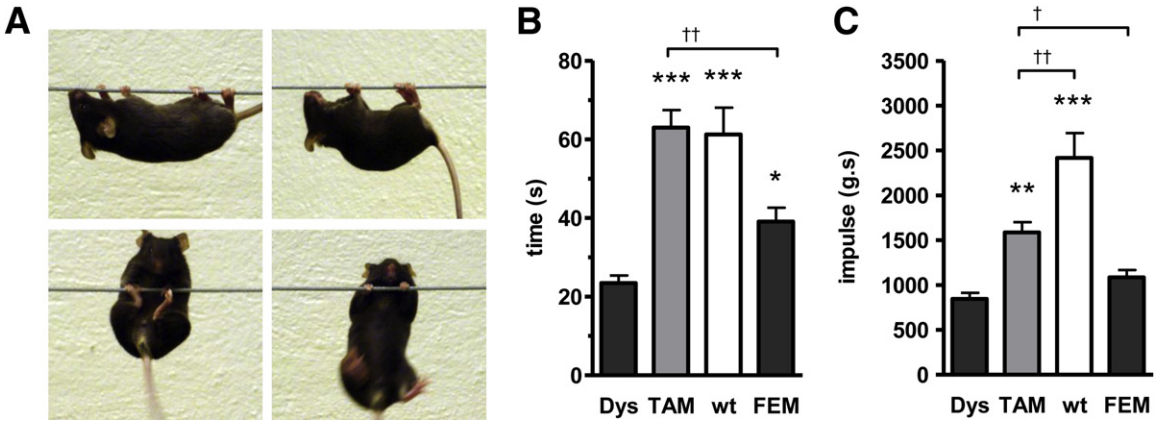

Figure 1 Effect of TAM treatment on the wire test score. A wire test was used to assess whole body force of male dystrophic mice (Dys), male dystrophic mice treated with 10 mg/kg per day of tamoxifen for 15 months (TAM), male wild-type mice (wt), and female dystrophic mice (FEM). **A:** Different views of a Dys mouse during the wire test. The mice were allowed to grasp a metal wire maintained horizontally above a thick layer of soft bedding. The Dys animals rapidly lost grip of their hind paws and hung onto the wire with their forelimbs only. From this position, they were unable to sustain their own body weight for more than a few seconds before falling. **B:** The length of time until the mice fell from the wire was recorded and showed that TAM normalized the ability of the dystrophic mice to maintain their grip. **C:** The physical impulse was calculated to take into account the smaller body weight of the dystrophic females and the TAM-treated males. The values represent means ± SEMs of 9 to 14 mice. $*P \leq 0.05$, $**P \leq 0.01$, $***P \leq 0.001$ compared with the Dys group; $^{\dagger}P \leq 0.05$, $^{\dagger\dagger}P \leq 0.01$ compared with the TAM group.

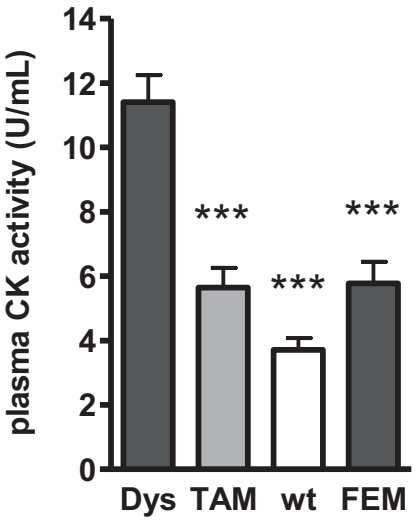

Figure 2 Effect of TAM treatment on plasma CK levels. Blood was collected from male dystrophic mice (Dys), male dystrophic mice treated with 10 mg/kg per day of tamoxifen for 15 months (TAM), male wild-type mice (wt), and female dystrophic mice (FEM). The plasma was prepared by centrifugation, and plasma CK levels were determined spectrophotometrically with the use of a commercial kit. The values represent means ± SEMs of 8 to 11 mice. ***$P \leq 0.001$ compared with the Dys group.

(Table 3 and Figure 3B). TAM treatment for 15 months conferred the triceps surae a much slower phenotype. Compared with the Dys group, the TTP value increased by 56% and the $RT_{1/2}$ value by 72% (Table 3 and Figure 3B). Accordingly, the rates of maximum tension development during contraction or of maximum tension loss during relaxation were 36% and 38% smaller, respectively (Table 3). Consistent with the slower contraction, the TAM group exhibited a marked leftward shift of the curve connecting the tension output to the frequency of stimulation (Figure 3D).

We next evaluated the resistance of the triceps surae against repeated tetanic contractions (Figure 3E). Previous studies from our laboratory suggested that this drastic assay showed the nonrecoverable fragility of the muscle toward damaging contractions rather than fatigue resulting, for instance, from limitation in oxygen supply or changes in the redox balance.[31] The tricep muscles of the Dys group showed a sharp loss of force as the tetani were repeatedly delivered. The normal mice were significantly more resistant during the first 15 tetani, until their force dropped and became similarly low as in the Dys group (Figure 3E). The dystrophic females exhibited increased resistance compared with the dystrophic males. TAM treatment for 15 months caused the triceps to lose force at a lower rate than in the untreated Dys group (Figure 3E). After a few tetani, the resistance of the TAM group to contraction-induced loss of force showed a significant improvement compared with the Dys group. Of note, the muscle resistance of the TAM group closely paralleled that of the FEM group (Figure 3E). The force drop index was calculated as the average difference between the experimental values and the response elicited by the first tetanus. The loss of force in the TAM and FEM groups was significantly less than that of the Dys and wt groups (Figure 3F).

Effects of TAM Treatment on Leg Muscle Structure

Examination of sections of EDL, soleus, and TA muscles stained with H&E or wheat-germ agglutinin showed in the Dys group well-known dystrophic changes, such as fibers with centrally located nuclei, indicative of muscle fiber regeneration, and excessive connective tissue. Exhaustive morphometric analyses showed that TAM caused diverse effects on different muscles with respect to centronucleated fibers, fibrosis, number of myofibers, and myofiber size (Supplemental Figures S2 and S3).

Effects of TAM Treatment on Diaphragm Morphology

H&E and wheat germ agglutinin staining revealed that long-term TAM treatment improved the quality of the DIA (Figure 4A and B, and Supplemental Figure S2, J–L). Fibrosis was significantly reduced (−21%) by TAM treatment (Figure 4, B and C). Interestingly, DIA from TAM-treated Dys mice were significantly heavier (76%) and thicker (59%) than those of untreated Dys mice (Figure 4, D and E). Further analysis demonstrated that these DIAs presented a significantly higher number of fibers (67%) and more fiber layers (48%) (Figure 4, F–H). The number of centronucleated fibers was significantly increased (33%), suggesting that more regeneration occurred (Figure 4I). In addition, the mean fiber diameter was increased close to that of the wt mice (Figure 4J), and the fraction of muscle cells to the total muscle surface was increased (21%) (Figure 4C). When combining the increased thickness of the DIA with the increased surface occupied by the myofibers, TAM augmented the amount of contractile tissue in the DIA by 72%.

Effect of TAM Treatment on Heart Fibrosis

Fibrosis was ∼3.5 times higher in Dys hearts than in the wt hearts (3.04% and 0.87% of the heart cross-sections, respectively) (Figure 5, A–C). Cardiac fibrosis was similar in the FEM group and in the Dys group. After TAM treatment, fibrosis was reduced to 1.86% of the ventricular surface, showing that TAM prevented the development of fibrosis in dystrophic hearts by ∼53% (Figure 5C).

Effects of TAM Treatment on Fiber Type Distribution

Fiber typing was performed with fluorescent antibodies directed against specific MyHC isoforms. We found subtle differences in the distribution of MyHCs between the Dys and wt groups (Supplemental Figure S4, A–E). In all leg muscles tested, except the GAS muscle, TAM caused an accumulation of the type I fibers (fatigue-resistant,

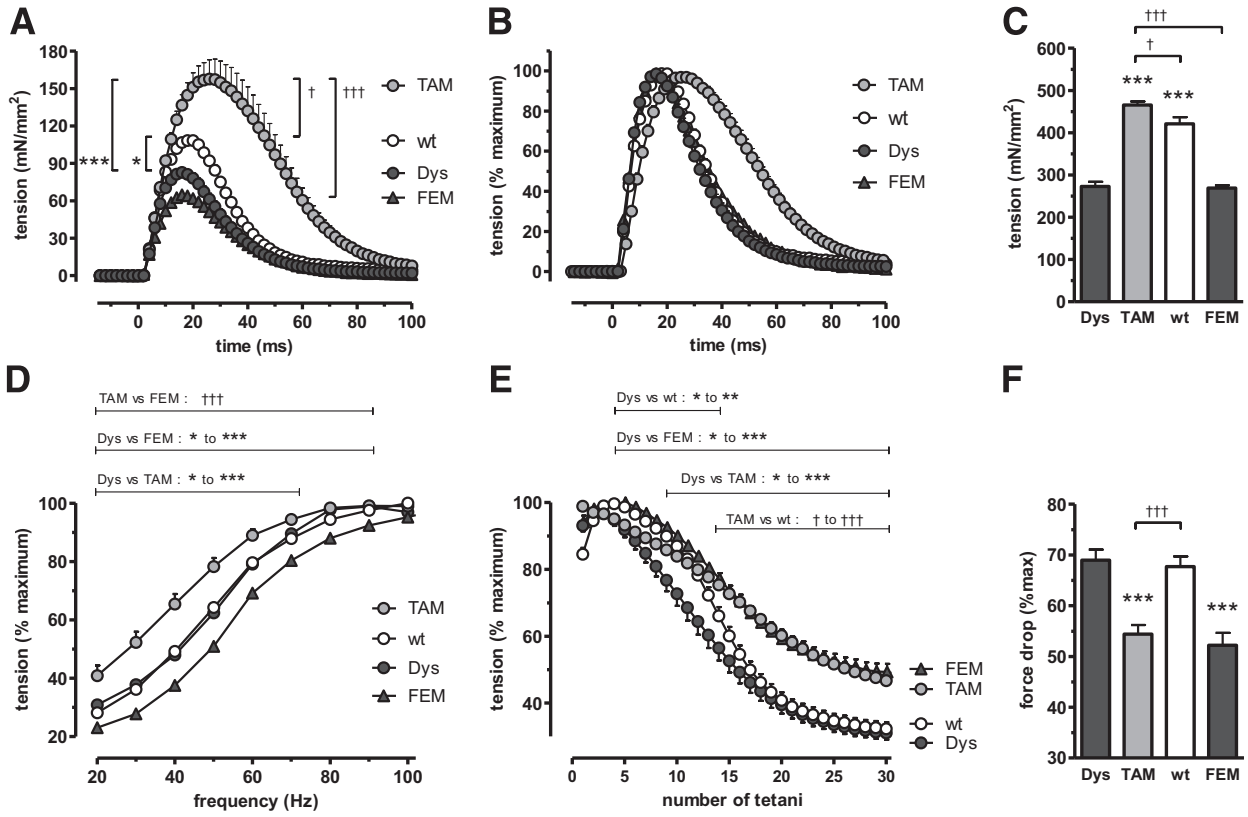

Figure 3 Effects of TAM treatment on the mechanical properties of the triceps muscle. Isometric force characteristics were determined on male dystrophic mice (Dys), male dystrophic mice treated with 10 mg/kg per day of tamoxifen for 15 months (TAM), male wild-type mice (wt), and female dystrophic mice (FEM). **A:** Phasic twitch traces normalized for muscle cross section showing that TAM-treated triceps developed much higher force than the other groups. **B:** Phasic twitch traces normalized to their maximum peak value, highlighting the slower kinetics of contraction and relaxation of TAM-treated triceps. **C:** Tetanic tensions normalized for muscle cross section showing that TAM-treated triceps were as strong as normal ones. **D:** Curves connecting the frequency of stimulation to muscle tension output, showing the slower contractile phenotype of the TAM-treated triceps. **E:** Loss of muscle tension on repeated tetanic contractions, showing that TAM made the triceps more resistant to fatigue. **F:** Average force drop calculated from the curves in E, showing that TAM prevented contraction-induced loss of force. The values represent means ± SEMs of 8 to 11 mice. $^{*}P \leq 0.05$, $^{**}P \leq 0.01$, and $^{***}P \leq 0.001$ compared with the Dys group; $^{\dagger}P \leq 0.05$, $^{\dagger\dagger}P \leq 0.01$, and $^{\dagger\dagger\dagger}P \leq 0.001$ compared with the TAM group.

slow-contracting fibers) or type IIA fibers (fatigue-resistant, fast-contracting fibers), with a concomitant reduction in the type IIX and IIB fibers (fatigue-sensitive, fast-contracting fibers). By contrast, the DIA showed an opposite response to TAM. As a result of these fiber type shifts, the ratio of types (I + IIA) to IIB fibers was normalized in the EDL, the soleus, the TA, and the DIA muscles of TAM-treated mice (Supplemental Figure S4, F–J).

Effects of TAM Treatment on the Expression of Muscle Markers

Proteins from GAS muscle extracts were analyzed by Western blot analysis. Their levels were corrected for MyHC content and normalized to the levels in the Dys group (Figure 6). Compared with the wt mice, the GAS muscle of the Dys mice contained significantly more utrophin, calsequestrin 2, SERCA2, and calcineurin but less calsequestrin 1. Treatment of Dys mice for 15 months with TAM significantly enhanced the expression of utrophin (+27%), α7 integrin (+36%), αB-crystallin (+61%), calsequestrin 2 (+39%), and calcineurin (+38%) and reduced the levels of parvalbumin (−35%), calsequestrin 1 (−28%), SERCA1 (−25%), and SERCA2 (−18%) (Figure 6, A–J).

Effects of TAM Treatment on Expression of ERs

The expression levels of ERα and ERβ were explored in the GAS muscle. RT-qPCR showed that ERα mRNA levels were similar in all groups (Figure 7A). In contrast, total ERβ mRNA levels were 2.3 times more abundant in the Dys mice than in the wt mice. These levels were further increased (+40%) by TAM treatment, resulting in ERβ mRNAs being 3.2 times higher than in the wt mice (Figure 7B). As shown by nested PCR with the use of primers flanking exon 7 (Figure 7C), the levels of ERβ1 mRNA, encoding the physiologically active ERβ subtype, were unchanged on TAM treatment. We found that the increase in ERβ mRNAs was mostly caused by the accumulation of the mRNA encoding ERβ2, a variant having an extended ligand-binding domain with lower affinity for estrogens (Figure 7D).[28,39] The ERβ2/ERβ1 mRNA

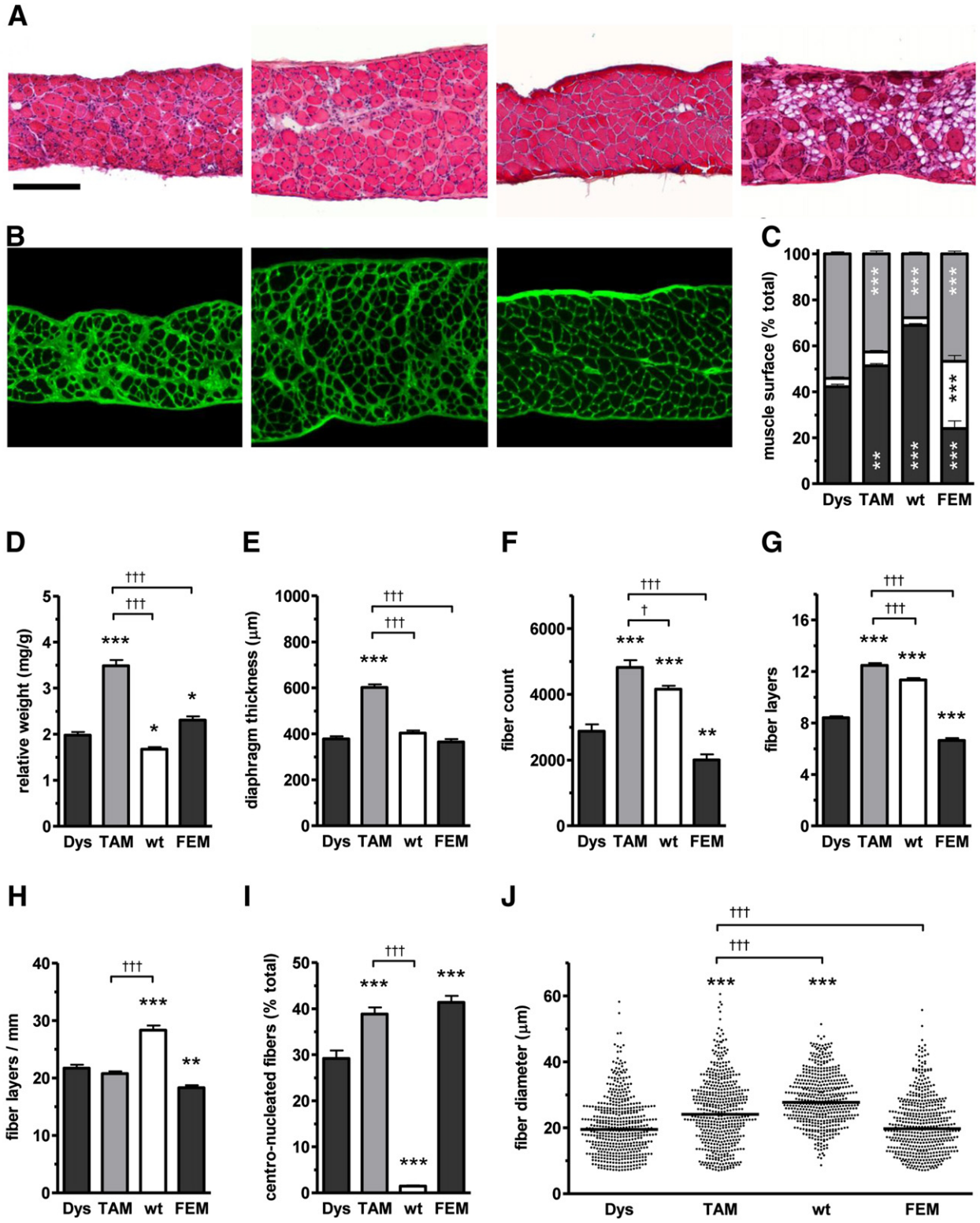

Figure 4 Effects of TAM treatment on diaphragm morphology. **A**: H&E-stained diaphragms from male dystrophic mice (Dys), male dystrophic mice treated with 10 mg/kg day of tamoxifen for 15 months (TAM), male wild-type mice (wt), and female dystrophic mice (FEM) (left to right). Scale bar = 200 µm. **B**: Fluorescent wheat germ agglutinin-stained diaphragms of the same groups as in **A**. The microphotograph of the FEM group was omitted. **C**: The surfaces occupied by myofibers (dark gray columns), connective tissue (light gray columns), and adipose tissue (white columns) were expressed as the percentage of the total diaphragm cross-sectional area. The relative weight (**D**), thickness (**E**), fiber number (**F**), and fiber layers (**G**) of the diaphragms were increased by TAM treatment. **H**: The number of fiber layers per millimeter was not changed by TAM, but an increase of centronucleated myofibers (**I**) and mean fiber diameter (**J**) was noted. For clarity, the scatter plots in J show the diameter of 500 individual fibers per group of >6000 fibers analyzed. The statistical analyses were performed on the total fiber populations. The values in **C**—**I** represent the means ± SEMs of 8 to 11 mice. $^{*}P \leq 0.05$, $^{**}P \leq 0.01$, and $^{***}P \leq 0.001$ compared with the Dys group; $^{\dagger}P \leq 0.05$, $^{\dagger\dagger\dagger}P \leq 0.001$ compared with the TAM group.

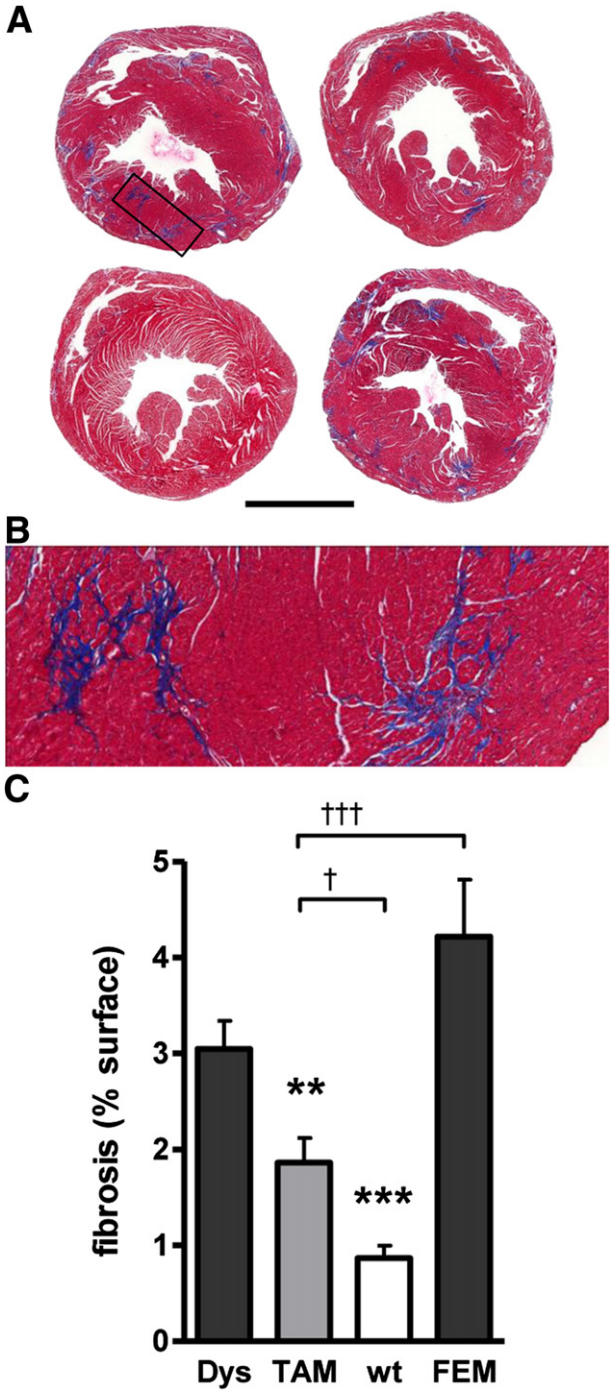

Figure 5 Effect of TAM treatment on heart fibrosis. Hearts were fixed in 4% buffered paraformaldehyde. After inclusion in paraffin sections (5 μm thick) across the ventricles were stained with Masson trichrome. The fibrotic deposits appear as a blue staining on a red background. **A**: Representative heart sections from a male dystrophic mouse (Dys) (**top left**), a male dystrophic mouse treated with 10 mg/kg per day of tamoxifen for 15 months (TAM) (**top right**), a female dystrophic mouse (FEM) (**bottom right**), and a male wild-type mouse (wt) (**bottom left**). **B**: Higher magnification view of the marked area in **A**, showing the fibrotic scars stained in blue. **C**: The areas stained blue were quantified and expressed as the percentage of the total tissue surface. Sections collected 1.50 mm, 2.25 mm, and 3.00 mm from the apex were analyzed and the values were averaged for every mouse. The values represent means ± SEMs of 8 to 11 mice. Scale bars: 2 mm (**A**); 400 μm (**B**). $^{**}P \leq 0.01$, $^{***}P \leq 0.001$ compared with the Dys group; $^{\dagger}P \leq 0.05$, $^{\dagger\dagger\dagger}P \leq 0.001$ compared with the TAM group.

ratio was seven times lower in Dys mice than in wt mice (Figure 7E). TAM treatment elevated the ERβ2/ERβ1 ratio more than fourfold, bringing it close to that of wt mice (Figure 7E). The mRNAs encoding shorter ERβ variants (ERβ5, ERβ5A, and ERβ6), which are expressed in the ovaries, were not detected in the GAS muscles from any group (Figure 7F). Western blot analysis showed that ERα and ERβ1 proteins were, respectively, 4.3 times and 3.5 times more abundant in Dys muscles than in wt muscles (Figure 7, G and H), whereas ERβ2 was expressed at similar levels in both groups (Figure 7I). TAM did not modify ERα and ERβ1 protein expression but caused a fourfold accumulation of the ERβ2 isoform in dystrophic muscle (Figure 7I), resulting in complete normalization of the relative ERβ2/ERβ1 protein ratio (Figure 7J).

Levels of TAM and Its Metabolites in Plasma and Muscle

We determined the concentrations of the E and Z isomers of TAM and of three major TAM metabolites in the plasma and in the GAS muscle of the TAM group. Results and representative chromatographic profiles are shown in Table 4 and Supplemental Figures S5 and S6, respectively. TAM isomers were the major species, followed by 4-OH-TAM, 4-hydroxy-*N*-desmethyl-TAM (also known as endoxifen), and *N*-desmethyl-TAM isomers. The latter were below the limit of quantification of the assay for the plasma. The compounds were 9 to 20 times more abundant in the GAS muscle than in the plasma. The levels of TAM and its metabolites in the muscle and the plasma of the TAM-treated mice were in the low nanomolar range. Unexpectedly, these levels were up to two to three orders of magnitude lower than those found in the same tissues of patients with breast cancer under standard TAM treatment[41,42] or of normal mice and rats.[43] In addition, in our TAM-treated mice, the E and Z isomers were present in roughly similar quantities, which contrasts with humans treated for breast cancer whereby the E isomers are usually only present in trace amounts.[37,44] Of note, we analyzed the food pellets and ruled out a Z-to-E interconversion during the preparation and the storage of the modified chow.

Discussion

TAM, a first-generation SERM, administrated orally for 15 months at 10 mg/kg/day to *mdx*^{5Cv} mice caused remarkable muscular improvements: i) the ability of the mice to maintain their grip was increased, suggesting that the body musculature was able to develop more force; ii) the triceps surae, a large group of muscles in the leg, displayed a striking enhancement of contractile features; iii) the DIA, the most severely affected muscle in dystrophic mice, became bigger, contained more fibers, but less fibrotic deposits; and iv) the heart showed a significant reduction in the extent of

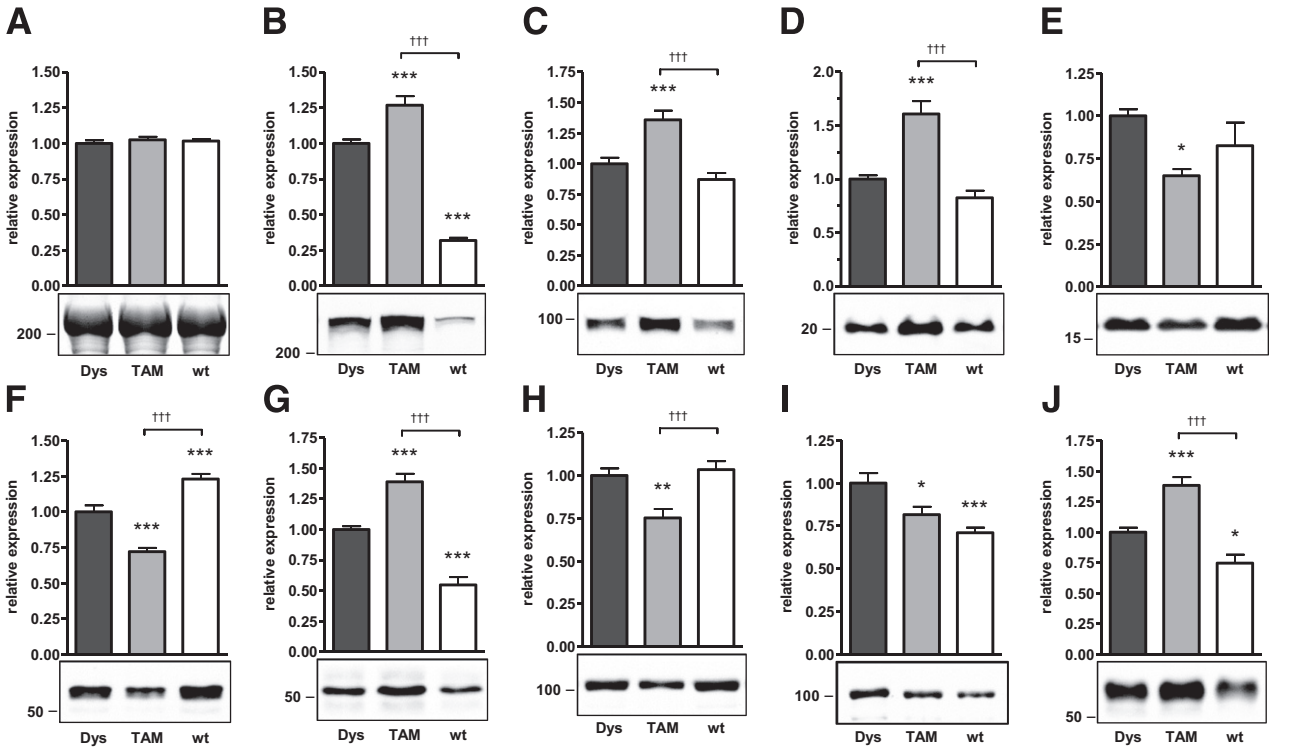

Figure 6 Effects of TAM treatment on the expression of muscle markers. Western blot analyses were performed on gastrocnemius extracts prepared from male dystrophic mice (Dys), male dystrophic mice treated with 10 mg/kg per day of tamoxifen for 15 months (TAM), and male wild-type mice (wt). **A**–**J**: The myosin heavy chains (**A**), shown by Coomassie Blue staining, were used for correcting the signals of the following muscle markers: utrophin (**B**), α7 integrin (**C**), αB-crystallin (**D**), parvalbumin (**E**), calsequestrin 1 (**F**), calsequestrin 2 (**G**), SERCA1 (**H**), SERCA2 (**I**), and calcineurin (**J**). The position of the molecular weight markers is indicated (in kDa). The values were normalized to the average value of the Dys group and represent the means ± SEMs of 11 mice per group. $^{*}P \leq 0.05$, $^{**}P \leq 0.01$, and $^{***}P \leq 0.001$ compared with the Dys group; $^{\dagger\dagger\dagger}P \leq 0.001$ compared with the TAM group.

fibrosis. To the best of our knowledge, this is the first report on the use of TAM on a model of muscular dystrophy.

Rationale for Using TAM

TAM and its active metabolites have been intensively studied for their ability to control survival, growth, and other functions of estrogen-dependent cell populations in the mammary glands, uterus, ovaries, and bones.[17–19,45] Apart from these effects, other actions, including prevention of oxidative stress,[20] protection against contraction-induced membrane damage,[14] modulation of calcium handling,[24–26] prevention of mitochondria-mediated cell death,[46] and inhibition of fibrosis[22,23,47] have been documented for TAM and its metabolites. These processes contribute to the pathogenic mechanisms at work in dystrophic muscle, and targeted interventions have been shown to improve the phenotype of dystrophic muscle to some extent.[7,31,33,35,48–51] Therefore, we reasoned that TAM should ameliorate the structure and the function of dystrophic muscles in mice. The findings described in the present report show that TAM remarkably ameliorated the function and the structure of murine dystrophic muscles.

All of the effects reported in the present study were obtained with tissue levels of TAM and its major metabolites much lower than those reported in prior studies on normal rodents.[43,52] In addition, we found that the E isomers accounted for an important part of the total TAM and metabolites. In humans, the unusual occurrence of high levels of the E isomers has been correlated with breast cancer resistance to TAM therapy and specific profiles of TAM-metabolizing cytochrome P450 enzymes.[53] More work is needed to clarify why the dystrophic mice display lower levels of TAM and its metabolites compared with normal mice[43] and high amounts of E isomers compared with humans.[37,44]

TAM Tolerability

As judged by the relative weight of selected organs and overall behavior, long-term administration of TAM to dystrophic mice was well tolerated. TAM significantly diminished the weight gain of the treated mice, which is likely because of the reduction of white fat. At the end of the treatment period, the TAM-treated males weighed the same as age-matched females.

Protective Actions of TAM on Muscle Function and Supporting Molecular Findings

Using several techniques, we have demonstrated that TAM ameliorates various force parameters of dystrophic muscle.

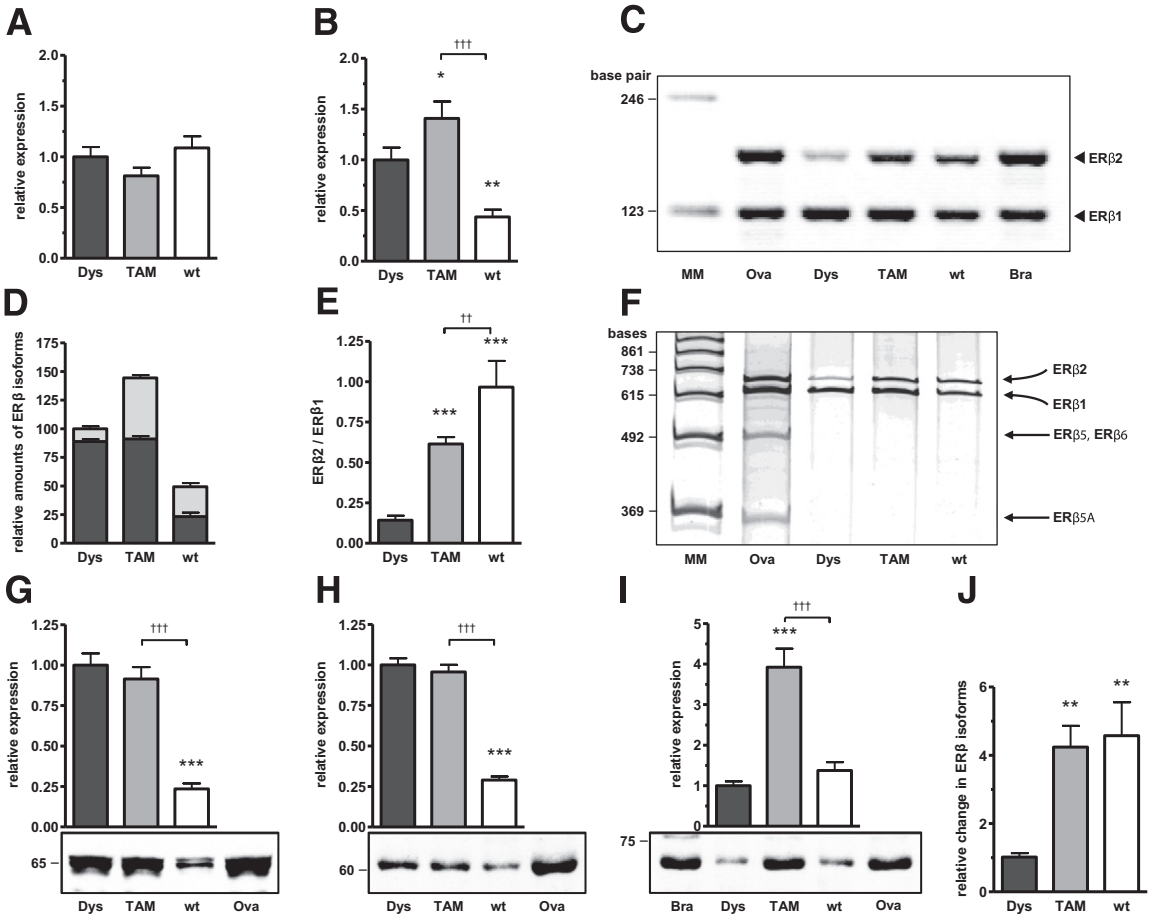

Figure 7 Effects of TAM treatment on the expression of estrogen receptors. Total protein and mRNA extracts were prepared from gastrocnemius muscles of male dystrophic mice (Dys), male dystrophic mice treated with 10 mg/kg per day of tamoxifen for 15 months (TAM), and male wild-type mice (wt). Brain (Bra) and ovary (Ova) extracts were included for comparison. The levels of ERα (**A**) and ERβ (**B**) mRNAs were determined by real-time qPCR. **C**—**E**: The relative abundance of the ERβ1 and ERβ2 isoforms were evaluated after nested PCR, followed by gel electrophoresis and densitometric analysis of the bands. **C**: Representative agarose gel, showing PCR amplification of the ERβ1 and ERβ2 isoforms. The molecular weight markers are shown (base pairs). **D**: Relative abundance of the ERβ1 and ERβ2 isoforms, normalized to the total ERβ content in the Dys group. **E**: ERβ2-to-ERβ1 mRNA ratio. **F**: Denaturing urea-polyacrylamide gel electrophoresis showed that gastrocnemius muscles did not express small ERβ isoforms (ERβ5, ERβ5A, ERβ6) that can be found in ovaries (**arrows**). The molecular weight markers are shown (bases). Western blot quantification of ERα (**G**), ERβ1 (**H**), and ERβ2 (**I**). The position of the molecular weight markers is indicated (in kDa). **J**: ERβ2-to-ERβ1 protein ratio normalized to the values of the Dys group. The data represent the means ± SEMs of 11 mice per group. $^{*}P \leq 0.05$, $^{**}P \leq 0.01$, and $^{***}P \leq 0.001$ compared with the Dys group; $^{\dagger\dagger}P \leq 0.01$, $^{\dagger\dagger\dagger}P \leq 0.001$ compared with the TAM group.

The wire test, like other hanging tests, is a rather stringent assay that challenges many muscles simultaneously, including those of the limbs as well as the trunk, abdominal, and back muscles.[40] The much-increased score at the wire test showed that TAM greatly improved overall muscle function of active dystrophic mice. This score could be affected by changes in force, fatigability, and possibly also balance. Therefore, we extended the evaluation of muscle function with the use *in situ* isometric contractions of the triceps surae, a large muscle group of the lower leg that is representative of most locomotor muscles. In agreement with the grid test findings, we found that the P_t and the P_o developed per unit of muscle cross section were much higher in the TAM-treated triceps than in triceps from untreated dystrophic mice. In addition, and as shown by longer TTP and $RT_{1/2}$ and smaller maximum rates of tension development and tension loss, TAM conferred much slower contraction kinetics to the triceps surae. The resistance of muscle to repeated tetanic contractions was also much higher in TAM-treated mice than in wt mice.

It has been established by others that the transient estrogen rise during the menstrual cycle correlates with enhanced muscle force,[12] and in certain paradigms estrogens conferred slower contraction and relaxation rates to the muscles,[12,54] involving either an alteration in calcium handling[54] or a decrease in type IIB fibers.[55]

TAM made dystrophic muscles even stronger than wt muscles, which one may find surprising. By contrast to what is expected with strategies aimed at re-introducing the missing dystrophin,[8] the mechanisms of action of active pharmacologic compounds do not necessarily involve the restoration of impaired signaling pathways and homeostatic

Table 4 Levels of TAM and its metabolites in plasma and gastrocnemius muscle

	Plasma		Gastrocnemius	
Compounds	ng/mL	nmol/L	ng/g	nmol/L
(Z)-tamoxifen	1.25 ± 0.30	3.35 ± 0.80	20.18 ± 4.58	54.32 ± 12.32
(E)-tamoxifen	1.75 ± 0.14	4.71 ± 0.38	16.01 ± 1.87	43.11 ± 5.02
(Z)-4-hydroxytamoxifen	1.22 ± 0.37	3.14 ± 0.97	13.31 ± 4.11	34.35 ± 10.60
(E)-4-hydroxytamoxifen	1.39 ± 0.11	3.59 ± 0.28	14.81 ± 2.06	38.23 ± 5.30
(Z)-*N*-desmethyl-tamoxifen	0.13 ± 0.03	0.37 ± 0.09	2.49 ± 0.50	6.96 ± 1.40
(E)-*N*-desmethyl-tamoxifen	0.30 ± 0.04	0.84 ± 0.10	3.69 ± 0.42	10.31 ± 1.16
(Z)-endoxifen	0.29 ± 0.05	0.78 ± 0.13	5.04 ± 0.83	13.49 ± 2.21
(E)-endoxifen	0.19 ± 0.02	0.51 ± 0.06	3.82 ± 0.49	10.22 ± 1.32

Values represent mean ± SEM of either 8 plasma or 11 muscles from TAM-treated mice. The plasma values for (Z) and (E)-*N*-desmethyl-tamoxifen are below the limit of quantification of the method and are shown for reference only.

balances back to normal levels. Moreover, it should be noted that the force developed by unexercised normal muscle does not represent an absolute upper limit that can in no condition be reached or exceeded. Instead, the force of normal muscles can be augmented by several conditions, including the use of doping substances and exercise that causes muscles to display an optimal redox balance and to ensure adaptation to the novel energy demand and structural requirements.[56–59] We suggest that TAM may have triggered and enhanced alternative pathways and compensatory mechanisms that could collectively ameliorate dystrophic muscle function and force output, possibly to levels above those of wt muscle.

Our findings of a slower rate of contraction and an enhanced resistance to fatigue in muscles from TAM-treated mice are of significance for the pathophysiology of muscular dystrophy. We established that the slower twitches resulted from a fast-to-slow fiber type shift and were accompanied by a molecular signature typical of slow-contracting muscles:

First, the slow-twitch phenotype is partly governed by the protein phosphatase calcineurin.[60] Our finding that TAM enhanced calcineurin expression in the GAS muscle suggests a fast-to-slow phenotype transition. This is in agreement with data showing that chronic activation of calcineurin in normal skeletal muscle promoted fast-to-slow fiber transition, increased endurance, improved resistance to fatigue, and enhanced mitochondrial oxidative function.[61,62] In support of a protective role for calcineurin in dystrophic muscle, reports indicate that inhibition of calcineurin activity by cyclosporin A aggravated the *mdx* phenotype, whereas constitutively active calcineurin protected *mdx* muscles from damage.[63]

Second, it is established that the fast-contracting type IIB fibers of both patients with DMD and *mdx* mice are more susceptible to damage than the slow-twitch type I fibers.[64,65] This might be because of higher antioxidant defense mechanisms and accumulation of utrophin, a dystrophin homologue, in slow compared with fast fibers.[66] The EDL, TA, and soleus muscles of the TAM-treated mice contained an increased number of type I fibers or of fast-twitch, fatigue-resistant type IIA fibers and, consequently, displayed an increased value of the (I + IIA)/IIB fiber ratio, which was restored to normal. This index was also normalized in the DIA, although this was achieved through a relative reduction of the type I and IIA fibers, which might result from a protection of the fragile type IIB fibers in that muscle.

Third, fiber type shift did not occur in the GAS muscle because the (I + IIA)/IIB fiber index was similar in all groups, which is in agreement with studies by others showing similar fiber type compositions in normal and dystrophic GAS muscle.[67] However, Western blot analyses showed changes in the levels of calcium handling proteins, again suggestive of a transition toward a slower phenotype. The GAS muscle from TAM-treated mice contained more of the slow type–specific protein calsequestrin-2 together with reduced levels of the fast type–specific proteins SERCA1, calsequestrin-1, and parvalbumin (reviewed in Berchtold et al[68] and Reggiani and Kronnie[69]). SERCA2 levels in dystrophic GAS muscle were also reduced by TAM close to normal amounts. Interestingly, SERCA2 was found to be overexpressed in the fast-twitch EDL muscle in *mdx* mice, likely as a compensatory mechanism.[70] We suggest that the TAM-induced reduction of SERCA2 in GAS muscle might result from an alleviation of the dystrophic symptoms.

We have also established that TAM treatment enhanced the accumulation of several structural proteins, such as the dystrophin homologue utrophin, α7 integrin, and αB-crystallin. When overexpressed in *mdx* mice, utrophin and α7 integrin have proven to be of therapeutic interest by acting as surrogates for the missing dystrophin.[32,71,72] αB-crystallin is a small heat shock protein that is much more abundant in slow-twitch than in fast-twitch muscles.[73] It acts as a chaperone for several myofibrillar proteins such as desmin, a muscle-specific intermediate filament that is critical for maintaining the integrity of the myofilaments, and for ensuring their proper anchoring to other binding partners.[73] Of note, mutations in either desmin or αB-crystallin result in a variety of muscular disorders.[74] In support of a protective role for TAM-induced accumulation

of structural proteins, recent studies reported that up to 20% of the force deficit in old *mdx* mice is due to altered myofilament architecture[75] and that reciprocally damaging contractions impair myofilament activity.[76] Taken individually, the overexpression level of every one of these structural proteins is likely too low to promote significant protection. We suggest that their simultaneous overexpression contributed to the TAM-induced increase of muscle force and to the recovery of membrane stability.

Altogether, the fiber type shifts, the increased levels of calcineurin, the accumulation of various structural proteins, and the alterations in calcium handling proteins suggest that TAM triggered complex transcriptional programs that protected the muscle, at least partly, via the acquisition of a slower and fatigue-resistant phenotype.[60,62]

Protective Actions of TAM on Overall Muscle Structure

Most muscles of the mdx^{5Cv} mouse undergo massive necrosis at ~3 to 5 weeks of age, followed by the formation of new myofibers retaining internal nuclei and displaying an important scattering of their diameter. From 8 to 10 weeks of age, the degeneration-regeneration cycles continue at a lower rate, and at ~1 year of age, as the self-repair capabilities of the muscle decline, connective tissue infiltration becomes prominent. In young dystrophic mice, centronucleated fibers are a reliable marker of the proportion of fibers that have disappeared due to prior necrosis.[31,34,51] In the present study, the interpretation of centronucleation is complicated by the long duration of treatment, during which the muscles likely underwent several cycles of necrosis-regeneration, and by the fact that the regenerated fibers are more vulnerable than the original ones.[77] However, it is likely that the decreased centronucleation in the soleus and the TA muscles is subsequent to prevention of necrosis and that the increased proportion of regenerated fibers in the EDL muscle and the DIA results from enhanced regeneration. This view is strongly supported by the relative weights of these muscles, the alteration of which parallels the centronucleation index. Whether these muscle-specific effects correlate with different expression profiles of the ERs and/or their nuclear cofactors in different muscles remains to be established. This possibility finds some support from earlier work to suggest higher ER levels in slow-twitch muscles from rabbit[78] as well as from recent findings from Feder et al[79] who found altered ER expression in EDL and quadriceps muscles of *mdx* mice (D. Feder, personal communication).

Normalization of myofiber size, reduction of the scattering of myofiber diameter, and decreased fibrosis are considered positive outcomes in the evaluation of therapeutic interventions in older dystrophic mice. Overall, several muscles from both the anterior and the posterior lower leg as well as the DIA showed a favorable evolution of one or more of these parameters with TAM. We believe that most of the musculature benefited similarly from TAM exposure, which is supported by the enhanced performance at the wire test.

Protective Actions of TAM on Diaphragm and Heart

TAM has been shown to prevent fibroblast activation, decrease collagen synthesis, and inhibit the release of transforming growth factor (TGF)-β, a major profibrotic mediator, in several conditions such as keloids, rhinophyma, Dupuytren disease, and retroperitoneal fibrosis.[22,23,47,80] Here, we demonstrate that TAM decreased the progression of fibrosis in the dystrophic heart and DIA. Furthermore, TAM showed additional protective effects on the DIA. It ameliorated the myofiber diameter, increased the proportion of regenerated fibers, and greatly enhanced the thickness of the muscle, which resulted mostly from an increase in the total number of myofibers. After TAM treatment, the net amount of tissue consisting of myofibers likely to contribute to the respiratory function was augmented by 72%. Collectively, these results suggest that TAM alleviated the muscular dystrophy in the DIA and strongly promoted the formation of new myofibers. In support of this, we found that the plasma level of TGF-β, a growth factor that controls muscle regeneration and fibrosis, was reduced (unpublished data). The DIA is the muscle of the dystrophic mouse that best mirrors the human condition.[81] Several pharmacologic interventions, such as immunosuppressors, green tea polyphenols, and blockers of TGF-β signaling pathways, reduced fibrosis in the DIA.[51,82,83] Other substances (reviewed in Judge et al[5]), such as halofuginone and deflazacort (but not prednisolone), were found efficacious for ameliorating cardiac function or reducing cardiac fibrosis. Together with losartan,[50] TAM appears to be one of the few compounds that reduces the development of fibrotic scars in both the DIA and the heart of dystrophic mice. This may be related to their common ability to reduce TGF-β. Improving respiratory and cardiac functions is a challenging issue for ameliorating the quality of life and increasing the life expectancy of patients with DMD.[4,5] This makes TAM particularly attractive as a therapeutic agent for treating muscular dystrophy.

Significance of ER Expression and Low Levels of TAM and Metabolites in Muscle

Natural estrogens and TAM are lipophilic compounds that accumulate in biological membranes, where they are thought to exert a variety of actions that involve neither ER nor transcription. In *in vitro* systems, short-term exposure to high concentrations of TAM were found to increase membrane fluidity,[84] to protect phospholipids from peroxidation[20] and to directly modulate the activity of ion channels and pumps.[24–26] Typically, these effects were seen with 1 to 20 μmol/L TAM in the extracellular fluid, which likely leads to much higher local concentrations in the membranes of the cultured cells. Several pharmacodynamic

studies on normal mice and rats reported that TAM and its metabolites reach concentrations in the low micromolar range in various tissues, including skeletal muscle.[43,52] Our findings show that the total concentration of TAM and its metabolites in the GAS muscle of dystrophic mice was ~200 nmol/L, which is likely insufficient for triggering physical actions on the membrane. Moreover, data from others suggest that direct membrane actions of TAM would not prevail *in vivo*. Koot and colleagues[14] reported that TAM-induced protection of rat skeletal muscles from damaging contractions was achieved after long-term treatment, whereas short-term (24 hours) treatment was ineffective. Therefore, we believe that the decreased CK value that we report here is the consequence of ER-dependent mechanisms that lead to myofiber stabilization rather than a direct effect on membrane fluidity or stability. In fact, we have recently demonstrated that doses of TAM as low as 0.1 mg/kg/day (ie, 100 times lower than the dose used in the present study) still produced significant improvements of most motor endpoints, lowered plasma CK levels, and reduced the number of Evans blue dye-permeable fibers and that TAM actions were antagonized by the ER blocker fulvestrant (O.M. Dorchies et al, manuscript in preparation), which provides strong support for receptor-mediated effects of TAM on dystrophic muscle.

Most of the effects of estrogens, TAM, and TAM metabolites result from their high-affinity binding to ERα and ERβ that are expressed in estrogen-responsive tissues of both males and females, including skeletal muscle.[10,11,28] Several ERβ isoforms exist. ERβ1 is considered as the physiologically active isoform, whereas ERβ2, a longer isoform with much reduced affinity for estrogens, would act in a dominant negative manner for the other ERs.[27,28] We report here, for the first time, that dystrophic muscle is enriched in both ERα and ERβ. This could well be the underlying reason for the unexpectedly high responsiveness of this tissue to TAM. Moreover, we found that the imbalance in the relative amounts of ERβ1 and ERβ2 tended to be normalized by TAM due to increased expression of ERβ2. This is particularly interesting in light of recent studies that demonstrate a role for ERβ in preventing both hypertrophy and fibrosis of the heart,[85,86] although these studies do not allow distinguishing the roles of different ERβ isoforms. Previous work by others have suggested that ER are expressed in various cell types within mammalian skeletal muscle, including endothelium, myoblasts, and myofibers.[10,11] In our hands, immunofluorescence labeling of mouse muscle tissues with the use of a large number of commercially available antibodies produced inconsistent staining patterns (data not shown). Consequently, more work is needed to unequivocally identify the cell type(s) that convey the increased ER expression in dystrophic skeletal muscles.

After binding their ligands, homodimers or heterodimers of ERα/ERβ regulate the transcription of target genes that bear palindromic estrogen-response elements in their promoter regions.[87] We have screened for the presence of estrogen-response elements in the upstream regions of the genes encoding several of the proteins whose expression was altered by TAM treatment. Although no complete estrogen-response element was found, these regions bear many estrogen-response element half-sites, which, in certain instances, may suffice to control the expression of estrogen target genes.[87] More experiments are needed to establish if TAM stimulated the expression of these proteins through increased transcription.

Tissue-specific estrogen sensitivity and response to TAM are essentially defined by the pattern of expression of ERα, ERβ, co-activators, and co-repressors. On binding to ERα or ERβ, TAM alters the set of co-regulators that are recruited, resulting in either proestrogenic or antiestrogenic effects in a tissue-specific manner.[28] Several of our findings suggest that TAM mimics estrogens on skeletal muscle. TAM increased the force and the resistance to fatigue and slowed the kinetics of contraction. Moreover, TAM-treated males weighed the same as age-matched females, most muscles from both groups had similar relative weights, and their plasma CK levels were similarly low. However, major differences remained between TAM-treated males and untreated females. As judged by the physical impulse scores determined from the wire hanging test and by the phasic and tetanic forces, the females were as weak as the untreated males, the female DIA accumulated much more adipose tissue, and both the female DIA and heart were not protected against fibrosis. Therefore, although our results indicate that TAM exerted protective effects on the overall musculature, this compound does not just "feminize" skeletal muscles of dystrophic mice nor does it fully mimic the natural estrogens. In fact, TAM binding to ER results in either proestrogenic or antiestrogenic actions, depending on the cell type,[19] which is characteristic of many SERMs, whereas natural estrogens elicit proestrogenic responses only. In addition, TAM and natural estrogens may modulate ER-independent pathways in a different manner,[24–26,88] resulting in distinct biological responses. Of note, it is likely that the levels of circulating estrogens were reduced in the relatively old females used in this study.

The issue of whether TAM is proestrogenic or antiestrogenic for dystrophic muscle is currently under investigation in our laboratory. This is complicated by the fact that several TAM metabolites exhibit a 30- to 100-fold higher affinity for ERs and display a stronger antiestrogenic activity than the parental drug and that the (E)-isomers display much lower antiestrogenic activity than the (Z)-isomers, at least as evaluated on breast cancer cells.[89] The use of other SERMs, such as raloxifene, whose biological activity does not depend on metabolites, might be useful for clarifying the roles of estrogen signaling in dystrophic muscle function. However, current work in our laboratory shows that raloxifene is much less efficacious than TAM on mdx^{5Cv} mice (O.M. Dorchies et al, manuscript in preparation).

Potential of TAM for DMD and Other Dystrophies

Over the past years, considerable efforts have been made toward therapies that replace or repair the defective dystrophin gene and permit the production of quasi-dystrophin.[8] However, technologic, cost, and safety issues obstruct the development of these approaches. In our view, the evaluation of known orally active small-molecular weight compounds with well-characterized pharmacodynamic and safety profiles presents significant advantages over other therapeutic avenues.[7] In particular, they might provide benefit to patients with DMD within a minimum period of time and are much less costly.

Our study suggests that TAM might be well-suited for this purpose. Besides its good safety profile in adults,[17–19,90] several studies report that it was also well tolerated when given for up to 48 months to 13-to 16-year-old prepubertal boys and for 12 months to girls as young as 3 years.[45,91,92] Importantly, in these studies, TAM did not alter the acquisition of male sexual traits. However, no data exist about the safety of TAM on growing boys as young as 5 to 7 years of age, at the time when the disease is diagnosed and treatment is likely to be initiated. This limitation should be taken into account if TAM is being evaluated on young patients with DMD.

Patients with DMD under usual steroid medications exhibit reduced growth and altered bone quality, which correlates with more frequent fractures. However, the reduction of the stature might participate in the therapeutic benefits of steroids (see Bianchi et al[93] and references within). By contrast, TAM prevents bone loss[17,94] and has been shown to increase the height of short boys by decreasing the rate of bone maturation.[92] At present, it is not known whether the foreseen action of TAM on stature might be a therapeutic issue for boy with DMD.

Our study shows that very low levels of TAM and TAM metabolites are sufficient to cause major therapeutic effects on the dystrophic mouse, which is encouraging in the perspective of a clinical application of our findings to patients with DMD. It is possible that therapeutic TAM concentrations might be reached with lower than standard TAM regimen, the safety of which has been established for more than 20 years. The specific benefits elicited by the E isomers of TAM metabolites, which were produced in substantial amounts in the dystrophic mice but are barely detected in humans,[37,44] deserve further examination. This could result in lower than expected benefits when extrapolating our results from mice to patients with DMD.

In conclusion, our preclinical evaluation of TAM in a mouse model of DMD showed promising improvements of skeletal and cardiac muscles. However, more investigations are required to establish the actions of TAM on further aspects of the dystrophic disease, such as the prevention of the initial muscle necrosis and the modulation of the inflammatory responses. Our further work will also aim at elucidating the molecular mechanisms that underlie the actions of TAM on dystrophic skeletal muscle, in particular with respect to the signaling pathways, the contributions of the ERs, and the specific activities of TAM metabolites.

Acknowledgments

We thank Colette Sauty-Defferard for animal care and excellent technical support, the other members of the laboratory for helpful discussions, and Prof. Randall Kramer (University of California, San Fransisco, CA) for the kind gift of anti-α7 integrin antibody. The BA-D5, SC-71, BF-35, and BF-F3 hybridoma developed by Prof. Stefano Schiaffino were obtained from the Developmental Studies Hybridoma Bank developed under the auspices of the National Institute of Child Health & Human Development and maintained by The University of Iowa, Department of Biology (Iowa City, IA).

Supplemental Data

Supplemental material for this article can be found at *http://dx.doi.org/10.1016/j.ajpath.2012.10.018*.

References

1. Morrison LA: Dystrophinopathies. Handb Clin Neurol 2011, 101: 11–39
2. Whitehead NP, Yeung EW, Allen DG: Muscle damage in mdx (dystrophic) mice: role of calcium and reactive oxygen species. Clin Exp Pharmacol Physiol 2006, 33:657–662
3. Allen D, Gervasio O, Yeung E, Whitehead N: Calcium and the damage pathways in muscular dystrophy. Can J Physiol Pharmacol 2010, 88: 83–91
4. Spurney CF: Cardiomyopathy of Duchenne muscular dystrophy: current understanding and future directions. Muscle Nerve 2011, 44:8–19
5. Judge DP, Kass DA, Thompson WR, Wagner KR: Pathophysiology and therapy of cardiac dysfunction in Duchenne muscular dystrophy. Am J Cardiovasc Drugs 2011, 11:287–294
6. Manzur A, Kuntzer T, Pike M, Swan A: Glucocorticoid corticosteroids for Duchenne muscular dystrophy. Cochrane Database Syst Rev 2008;(1):CD003725
7. Fairclough RJ, Perkins KJ, Davies KE: Pharmacologically targeting the primary defect and downstream pathology in Duchenne muscular dystrophy. Curr Gene Ther 2012, 12:206–244
8. Verhaart IE, Aartsma-Rus A: Gene therapy for Duchenne muscular dystrophy. Curr Opin Neurol 2012, 25:588–596
9. Larionov AA, Vasyliev DA, Mason JI, Howie AF, Berstein LM, Miller WR: Aromatase in skeletal muscle. J Steroid Biochem Mol Biol 2003, 84:485–492
10. Wiik A, Ekman M, Morgan G, Johansson O, Jansson E, Esbjornsson M: Oestrogen receptor beta is present in both muscle fibres and endothelial cells within human skeletal muscle tissue. Histochem Cell Biol 2005, 124:161–165
11. Kalbe C, Mau M, Wollenhaupt K, Rehfeldt C: Evidence for estrogen receptor alpha and beta expression in skeletal muscle of pigs. Histochem Cell Biol 2006, 127:95–107
12. Sarwar R, Niclos BB, Rutherford OM: Changes in muscle strength, relaxation rate and fatiguability during the human menstrual cycle. J Physiol (Lond) 1996, 493(Pt 1):267–272

13. McClung JM, Davis JM, Wilson MA, Goldsmith EC, Carson JA: Estrogen status and skeletal muscle recovery from disuse atrophy. J Appl Physiol 2006, 100:2012−2023
14. Koot RW, Amelink GJ, Blankenstein MA, Bar PR: Tamoxifen and oestrogen both protect the rat muscle against physiological damage. J Steroid Biochem Mol Biol 1991, 40:689−695
15. Kallen AN, Pal L: Cardiovascular disease and ovarian function. Curr Opin Obstet Gynecol 2011, 23:258−267
16. Yang X-P, Reckelhoff JF: Estrogen, hormonal replacement therapy and cardiovascular disease. Curr Opin Nephrol Hypertens 2011, 20: 133−138
17. Vogel VG, Costantino JP, Wickerham DL, Cronin WM, Cecchini RS, Atkins JN, Bevers TB, Fehrenbacher L, Pajon ER, Wade JL III, Robidoux A, Margolese RG, James J, Lippman SM, Runowicz CD, Ganz PA, Reis SE, McCaskill-Stevens W, Ford LG, Jordan VC, Wolmark N: National Surgical Adjuvant Breast and Bowel Project (NSABP): Effects of tamoxifen vs raloxifene on the risk of developing invasive breast cancer and other disease outcomes. JAMA 2006, 295: 2727−2741
18. Vogel VG: The NSABP Study of Tamoxifen and Raloxifene (STAR) trial. Expert Rev Anticancer Ther 2008, 9:51−60
19. Singh MN, Martin-Hirsch PL, Martin FL: The multiple applications of tamoxifen: an example pointing to SERM modulation being the aspirin of the 21st century. Med Sci Monit 2008, 14:RA144−RA148
20. Custodio JB, Dinis TC, Almeida LM, Madeira VM: Tamoxifen and hydroxytamoxifen as intramembraneous inhibitors of lipid peroxidation. Evidence for peroxyl radical scavenging activity. Biochem Pharmacol 1994, 47:1989−1998
21. Custodio JB, Moreno AJ, Wallace KB: Tamoxifen inhibits induction of the mitochondrial permeability transition by Ca^{2+} and inorganic phosphate. Toxicol Appl Pharmacol 1998, 152:10−17
22. Kuhn MA, Wang X, Payne WG, Ko F, Robson MC: Tamoxifen decreases fibroblast function and downregulates TGFβ2 in Dupuytren's affected palmar fascia. J Surg Res 2002, 103:146−152
23. Payne WG, Ko F, Anspaugh S, Wheeler CK, Wright TE, Robson MC: Down-regulating causes of fibrosis with tamoxifen: a possible cellular/molecular approach to treat rhinophyma. Ann Plast Surg 2006, 56: 301−305
24. Dodds ML, Kargacin ME, Kargacin GJ: Effects of anti-oestrogens and beta-estradiol on calcium uptake by cardiac sarcoplasmic reticulum. Br J Pharmacol 2001, 132:1374−1382
25. Lobatón CD, Vay L, Hernández-SanMiguel E, SantoDomingo J, Moreno A, Montero M, Alvarez J: Modulation of mitochondrial Ca^{2+} uptake by estrogen receptor agonists and antagonists. Br J Pharmacol 2005, 145:862−871
26. Bolanz KA, Kovacs GG, Landowski CP, Hediger MA: Tamoxifen inhibits TRPV6 activity via estrogen receptor−independent pathways in TRPV6-expressing MCF-7 breast cancer cells. Mol Cancer Res 2009, 7:2000−2010
27. Chung WCJ, Pak TR, Suzuki S, Pouliot WA, Andersen ME, Handa RJ: Detection and localization of an estrogen receptor beta splice variant protein (ERbeta2) in the adult female rat forebrain and midbrain regions. J Comp Neurol 2007, 505:249−267
28. Heldring N, Pike A, Andersson S, Matthews J, Cheng G, Hartman J, Tujague M, Strom A, Treuter E, Warner M, Gustafsson J-A: Estrogen receptors: how do they signal and what are their targets. Physiol Rev 2007, 87:905−931
29. Nagaraju K, Willmann R: Developing standard procedures for murine and canine efficacy studies of DMD therapeutics: report of two expert workshops on "Pre-clinical testing for Duchenne dystrophy": Washington DC, October 27th-28th 2007 and Zürich, June 30th-July 1st 2008. Neuromuscul Disord 2009, 19:502−506
30. Beastrom N, Lu H, Macke A, Canan BD, Johnson EK, Penton CM, Kaspar BK, Rodino-Klapac LR, Zhou L, Janssen PML, Montanaro F: mdx^{5cv} mice manifest more severe muscle dysfunction and diaphragm force deficits than do mdx mice. Am J Pathol 2011, 179:2464−2474
31. Dorchies OM, Wagner S, Vuadens O, Waldhauser K, Buetler TM, Kucera P, Ruegg UT: Green tea extract and its major polyphenol (-)-epigallocatechin gallate improve muscle function in a mouse model for Duchenne muscular dystrophy. Am J Physiol Cell Physiol 2006, 290:C616−C625
32. Puttini S, Lekka L, Dorchies OM, Saugy D, Incitti T, Ruegg UT, Bozzoni I, Kulik AJ, Mermod N: Gene-mediated restoration of normal myofiber elasticity in dystrophic muscles. Mol Ther 2009, 17: 19−25
33. Hibaoui Y, Reutenauer-Patte J, Patthey-Vuadens O, Ruegg UT, Dorchies OM: Melatonin improves muscle function of the dystrophic mdx^{5Cv} mouse, a model for Duchenne muscular dystrophy. J Pineal Res 2011, 51:163−171
34. Reutenauer-Patte J, Boittin F-X, Patthey-Vuadens O, Ruegg UT, Dorchies OM: Urocortins improve dystrophic skeletal muscle structure and function through both PKA- and Epac-dependent pathways. Am J Pathol 2012, 180:749−762
35. Reutenauer J, Dorchies OM, Patthey-Vuadens O, Vuagniaux G, Ruegg UT: Investigation of Debio 025, a cyclophilin inhibitor, in the dystrophic mdx mouse, a model for Duchenne muscular dystrophy. Br J Pharmacol 2008, 155:574−584
36. Nakae Y, Dorchies OM, Stoward PJ, Zimmermann BF, Ritter C, Ruegg UT: Quantitative evaluation of the beneficial effects in the *mdx* mouse of epigallocatechin gallate, an antioxidant polyphenol from green tea. Histochem Cell Biol 2012, 137:811−827
37. Dahmane E, Mercier T, Zanolari B, Cruchon S, Guignard N, Buclin T, Leyvraz S, Zaman K, Csajka C, Decosterd LA: An ultra performance liquid chromatography−tandem MS assay for tamoxifen metabolites profiling in plasma: first evidence of 4′-hydroxylated metabolites in breast cancer patients. J Chromatogr B Analyt Technol Biomed Life Sci 2010, 878:3402−3414
38. Briguet A, Courdier-Fruh I, Foster M, Meier T, Magyar JP: Histological parameters for the quantitative assessment of muscular dystrophy in the mdx-mouse. Neuromuscul Disord 2004, 14: 675−682
39. Lu B, Leygue E, Dotzlaw H, Murphy LJ, Murphy LC, Watson PH: Estrogen receptor-β mRNA variants in human and murine tissues. Mol Cell Endocrinol 1998, 138:199−203
40. Carlson CG, Rutter J, Bledsoe C, Singh R, Hoff H, Bruemmer K, Sesti J, Gatti F, Berge J, McCarthy L: A simple protocol for assessing inter-trial and inter-examiner reliability for two noninvasive measures of limb muscle strength. J Neurosci Methods 2010, 186:226−230
41. Furlanut M, Franceschi L, Pasqual E, Bacchetti S, Poz D, Giorda G, Cagol P: Tamoxifen and its main metabolites serum and tissue concentrations in breast cancer women. Ther Drug Monit 2007, 29: 349−352
42. Madlensky L, Natarajan L, Tchu S, Pu M, Mortimer J, Flatt SW, Nikoloff DM, Hillman G, Fontecha MR, Lawrence HJ, Parker BA, Wu AHB, Pierce JP: Tamoxifen metabolite concentrations. CYP2D6 genotype, and breast cancer outcomes. Clin Pharmacol Ther 2011, 89: 718−725
43. Robinson SP, Langan-Fahey SM, Johnson DA, Jordan VC: Metabolites, pharmacodynamics, and pharmacokinetics of tamoxifen in rats and mice compared to the breast cancer patient. Drug Metab Dispos 1991, 19:36−43
44. Murdter TE, Schroth W, Bacchus-Gerybadze L, Winter S, Heinkele G, Simon W, Fasching PA, Fehm T, Eichelbaum M, Schwab M, Brauch H: Activity levels of tamoxifen metabolites at the estrogen receptor and the impact of genetic polymorphisms of phase I and II enzymes on their concentration levels in plasma. Clin Pharmacol Ther 2011, 89:708−717
45. Eugster EA, Rubin SD, Reiter EO, Plourde P, Jou H-C, Pescovitz OH: Tamoxifen treatment for precocious puberty in McCune-Albright syndrome: a multicenter trial. J Pediatr 2003, 143:60−66
46. Cardoso CM, Almeida LM, Custodio JB: 4-Hydroxytamoxifen is a potent inhibitor of the mitochondrial permeability transition. Mitochondrion 2002, 1:485−495

47. van Bommel EF, Hendriksz TR, Huiskes AW, Zeegers AG: Brief communication: tamoxifen therapy for nonmalignant retroperitoneal fibrosis. Ann Intern Med 2006, 144:101−106
48. Iwata Y, Katanosaka Y, Arai Y, Shigekawa M, Wakabayashi S: Dominant-negative inhibition of Ca^{2+} influx via TRPV2 ameliorates muscular dystrophy in animal models. Hum Mol Genet 2009, 18:824−834
49. Goonasekera SA, Lam CK, Millay DP, Sargent MA, Hajjar RJ, Kranias EG, Molkentin JD: Mitigation of muscular dystrophy in mice by SERCA overexpression in skeletal muscle. J Clin Invest 2011, 121: 1044−1052
50. Spurney CF, Sali A, Guerron AD, Iantorno M, Yu Q, Gordish-Dressman H, Rayavarapu S, van der Meulen J, Hoffman EP, Nagaraju K: Losartan decreases cardiac muscle fibrosis and improves cardiac function in dystrophin-deficient mdx mice. J Cardiovasc Pharmacol Ther 2011, 16:87−95
51. Nakae Y, Hirasaka K, Goto J, Nikawa T, Shono M, Yoshida M, Stoward PJ: Subcutaneous injection, from birth, of epigallocatechin-3-gallate, a component of green tea, limits the onset of muscular dystrophy in mdx mice: a quantitative histological, immunohistochemical and electrophysiological study. Histochem Cell Biol 2008, 129:489−501
52. Lien EA, Solheim E, Ueland PM: Distribution of tamoxifen and its metabolites in rat and human tissues during steady-state treatment. Cancer Res 1991, 51:4837−4844
53. Gao L, Tu Y, Wegman P, Wingren S, Eriksson LA: A mechanistic hypothesis for the cytochrome P450-catalyzed cis−trans isomerization of 4-hydroxytamoxifen: an unusual redox reaction. J Chem Inf Model 2011, 51:2293−2301
54. McCormick KM, Burns KL, Piccone CM, Gosselin LE, Brazeau GA: Effects of ovariectomy and estrogen on skeletal muscle function in growing rats. J Muscle Res Cell Motil 2004, 25:21−27
55. Piccone CM, Brazeau GA, McCormick KM: Effect of oestrogen on myofibre size and myosin expression in growing rats. Exp Physiol 2005, 90:87−93
56. Reid MB: Invited Review: redox modulation of skeletal muscle contraction: what we know and what we don't. J Appl Physiol 2001, 90:724−731
57. Hughson RL: Regulation of blood flow at the onset of exercise by feed forward and feedback mechanisms. Can J Appl Physiol 2003, 28: 774−787
58. Macintosh BR, Robillard ME, Tomaras EK: Should postactivation potentiation be the goal of your warm-up? Appl Physiol Nutr Metab 2012, 37:546−550
59. Kho AL, Perera S, Alexandrovich A, Gautel M: The sarcomeric cytoskeleton as a target for pharmacological intervention. Curr Opin Pharmacol 2012, 12:347−354
60. Mallinson J, Meissner J, Chang K.-C: Calcineurin signaling and the slow oxidative skeletal muscle fiber type. ch 2. In: International Review of Cell and Molecular Biology. Edited by Kwang W.J. Academic Press, 2009, pp. 67−101
61. Jiang LQ, Garcia-Roves PM, de Castro Barbosa T, Zierath JR: Constitutively active calcineurin in skeletal muscle increases endurance performance and mitochondrial respiratory capacity. Am J Physiol Endocrinol Metab 2010, 298:E8−E16
62. Sakuma K, Yamaguchi A: The functional role of calcineurin in hypertrophy, regeneration, and disorders of skeletal muscle. J Biomed Biotechnol 2010, 2010:721219
63. Stupka N, Plant DR, Schertzer JD, Emerson TM, Bassel-Duby R, Olson EN, Lynch GS: Activated calcineurin ameliorates contraction-induced injury to skeletal muscles of mdx dystrophic mice. J Physiol 2006, 575:645−656
64. Webster C, Silberstein L, Hays AP, Blau HM: Fast muscle fibers are preferentially affected in Duchenne muscular dystrophy. Cell 1988, 52: 503−513
65. Moens P, Baatsen PH, Marechal G: Increased susceptibility of EDL muscles from mdx mice to damage induced by contractions with stretch. J Muscle Res Cell Motil 1993, 14:446−451
66. Chakkalakal JV, Stocksley MA, Harrison MA, Angus LM, Deschenes-Furry J, St-Pierre S, Megeney LA, Chin ER, Michel RN, Jasmin BJ: Expression of utrophin A mRNA correlates with the oxidative capacity of skeletal muscle fiber types and is regulated by calcineurin/NFAT signaling. Proc Natl Acad Sci U S A 2003, 100: 7791−7796
67. Muller J, Vayssiere N, Royuela M, Leger ME, Muller A, Bacou F, Pons F, Hugon G, Mornet D: Comparative evolution of muscular dystrophy in diaphragm, gastrocnemius and masseter muscles from old male mdx mice. J Muscle Res Cell Motil 2001, 22: 133−139
68. Berchtold MW, Brinkmeier H, Muntener M: Calcium ion in skeletal muscle: its crucial role for muscle function, plasticity, and disease. Physiol Rev 2000, 80:1215−1265
69. Reggiani C, Kronnie T: RyR isoforms and fibre type-specific expression of proteins controlling intracellular calcium concentration in skeletal muscles. J Muscle Res Cell Motil 2006, 27:327−335
70. Divet A, Lompré AV, Huchet-Cadiou C: Effect of cyclopiazonic acid, an inhibitor of the sarcoplasmic reticulum Ca-ATPase, on skeletal muscles from normal and mdx mice. Acta Physiol Scand 2005, 184: 173−186
71. Perkins K, Davies K: The role of utrophin in the potential therapy of Duchenne muscular dystrophy. Neuromuscul Disord 2002, 12: S78−S89
72. Burkin DJ, Wallace GQ, Milner DJ, Chaney EJ, Mulligan JA, Kaufman SJ: Transgenic expression of $\alpha 7\beta 1$ integrin maintains muscle integrity, increases regenerative capacity, promotes hypertrophy, and reduces cardiomyopathy in dystrophic mice. Am J Pathol 2005, 166: 253−263
73. Larkins NT, Murphy RM, Lamb GD: Absolute amounts and diffusibility of HSP72. HSP25, and αB-crystallin in fast- and slow-twitch skeletal muscle fibers of rat. Am J Physiol Cell Physiol 2012, 302: C228−C239
74. Sanbe A: Molecular mechanisms of alpha-crystallinopathy and its therapeutic strategy. Biol Pharm Bull 2011, 34:1653−1658
75. Friedrich O, Both M, Weber C, Schürmann S, Teichmann MDH, von Wegner F, Fink RHA, Vogel M, Chamberlain JS, Garbe C: Microarchitecture is severely compromised but motor protein function is preserved in dystrophic mdx skeletal muscle. Biophys J 2010, 98: 606−616
76. Blaauw B, Agatea L, Toniolo L, Canato M, Quarta M, Dyar KA, Danieli-Betto D, Betto R, Schiaffino S, Reggiani C: Eccentric contractions lead to myofibrillar dysfunction in muscular dystrophy. J Appl Physiol 2010, 108:105−111
77. Head SI: Branched fibres in old dystrophic mdx muscle are associated with mechanical weakening of the sarcolemma, abnormal Ca^{2+} transients and a breakdown of Ca^{2+} homeostasis during fatigue. Exp Physiol 2010, 95:641−656
78. Saartok T: Steroid receptors in two types of rabbit skeletal muscle. Int J Sports Med 1984, 5:130−136
79. Feder D, Godoy IRB, Pereira MLG, Silva CS, Silvestre DN, Fonseca FLA, Carvalho AAS, Santos RA, Carvalho MHC: Hormonal receptors in skeletal muscles of dystrophic mice. J Biomed Biotechnol 2012, (in press)
80. Chau D, Mancoll JS, Lee S, Zhao J, Phillips LG, Gittes GK, Longaker MT: Tamoxifen downregulates TGF-beta production in keloid fibroblasts. Ann Plast Surg 1998, 40:490−493
81. Stedman HH, Sweeney HL, Shrager JB, Maguire HC, Panettieri RA, Petrof B, Narusawa M, Leferovich JM, Sladky JT, Kelly AM: The *mdx* mouse diaphragm reproduces the degenerative changes of Duchenne muscular dystrophy. Nature 1991, 352:536−539
82. Gosselin LE, McCormick KM: Targeting the immune system to improve ventilatory function in muscular dystrophy. Med Sci Sports Exerc 2004, 36:44−51
83. Taniguti APT, Pertille A, Matsumura CY, Neto HS, Marques MJ: Prevention of muscle fibrosis and myonecrosis in mdx mice by suramin, a TGF-β1 blocker. Muscle Nerve 2011, 43:82−87

84. Custodio JB, Almeida LM, Madeira VM: The anticancer drug tamoxifen induces changes in the physical properties of model and native membranes. Biochim Biophys Acta 1993, 1150:123−129
85. Pedram A, Razandi M, Lubahn D, Liu J, Vannan M, Levin ER: Estrogen inhibits cardiac hypertrophy: role of estrogen receptor-β to inhibit calcineurin. Endocrinology 2008, 149:3361−3369
86. Pedram A, Razandi M, O'Mahony F, Lubahn D, Levin ER: Estrogen receptor-β prevents cardiac fibrosis. Mol Endocrinol 2010, 24: 2152−2165
87. Gruber CJ, Gruber DM, Gruber IML, Wieser F, Huber JC: Anatomy of the estrogen response element. Trends Endocrinol Metab 2004, 15: 73−78
88. Zhang JJ, Jacob TJ, Valverde MA, Hardy SP, Mintenig GM, Sepulveda FV, Gill DR, Hyde SC, Trezise AE, Higgins CF: Tamoxifen blocks chloride channels. A possible mechanism for cataract formation. J Clin Invest 1994, 94:1690−1697
89. Goetz MP, Kamal A, Ames MM: Tamoxifen pharmacogenomics: the role of CYP2D6 as a predictor of drug response. Clin Pharmacol Ther 2007, 83:160−166
90. Hayes TG: Pharmacologic treatment of male breast cancer. Expert Opin Pharmacother 2009, 10:2499−2510
91. Derman O, Kanbur N, Kilic I, Kutluk T: Long-term follow-up of tamoxifen treatment in adolescents with gynecomastia. J Pediatr Endocrinol Metab 2008, 21:449−454
92. Kreher NC, Eugster EA, Shankar RR: The use of tamoxifen to improve height potential in short pubertal boys. Pediatrics 2005, 116:1513−1515
93. Bianchi ML, Biggar D, Bushby K, Rogol AD, Rutter MM, Tseng B: Endocrine aspects of Duchenne muscular dystrophy. Neuromuscul Disord 2011, 21:298−303
94. Starnes LM, Downey CM, Boyd SK, Jirik FR: Increased bone mass in male and female mice following tamoxifen administration. Genesis 2007, 45:229−235